Galactic cosmic ray origin and composition

Vincent Tatischeff (CSNSM, Orsay)

1. Galactic cosmic-ray origin: the supernova remnant paradigm
2. Supernovas and supernova remnants
3. Massive star clusters and superbubbles
4. Lessons from the cosmic-ray composition

1. Galactic cosmic rays and diffuse γ-rays

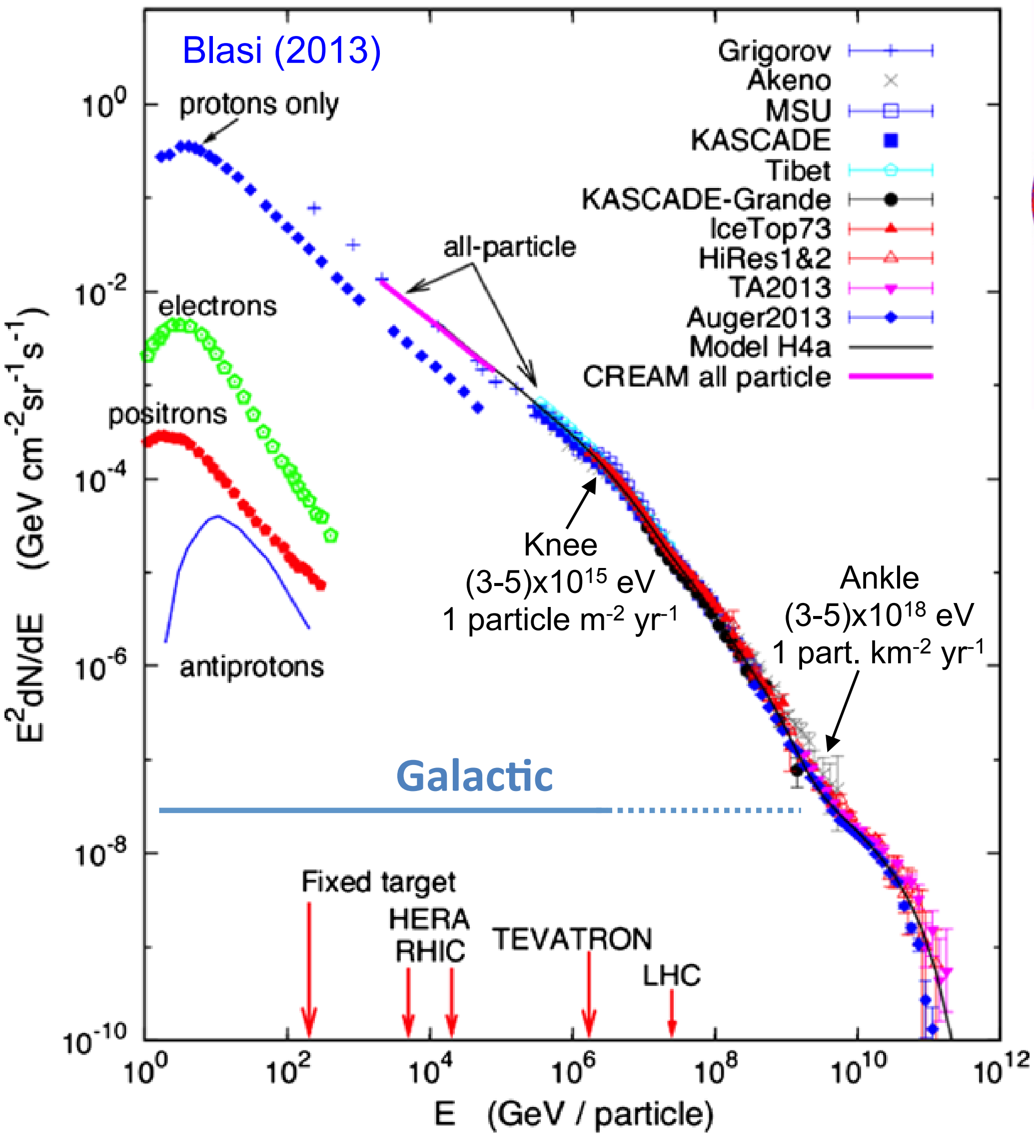

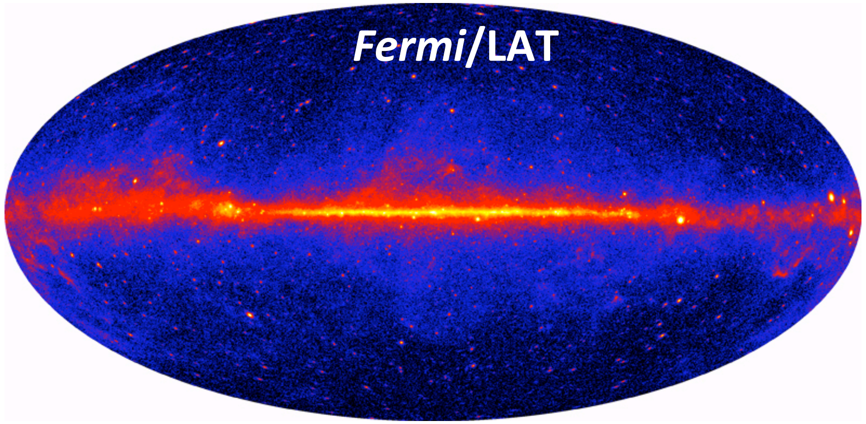

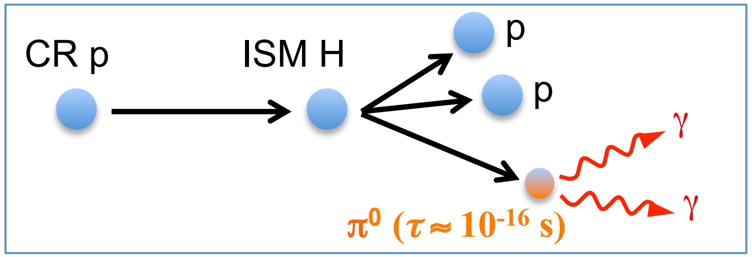

Gamma-ray (0.1 - 100 GeV) luminosity of the Galaxy (Strong et al. 2010):

- **π^0 decay (p+p->π^0): ~ 5×10^{38} erg/s**
- Inverse Compton: ~ 1.5×10^{38} erg/s
- Bremsstrahlung: ~ 0.5×10^{38} erg/s
- **Total**: ~ 7×10^{38} erg/s

1. Galactic cosmic-ray and supernova energetics

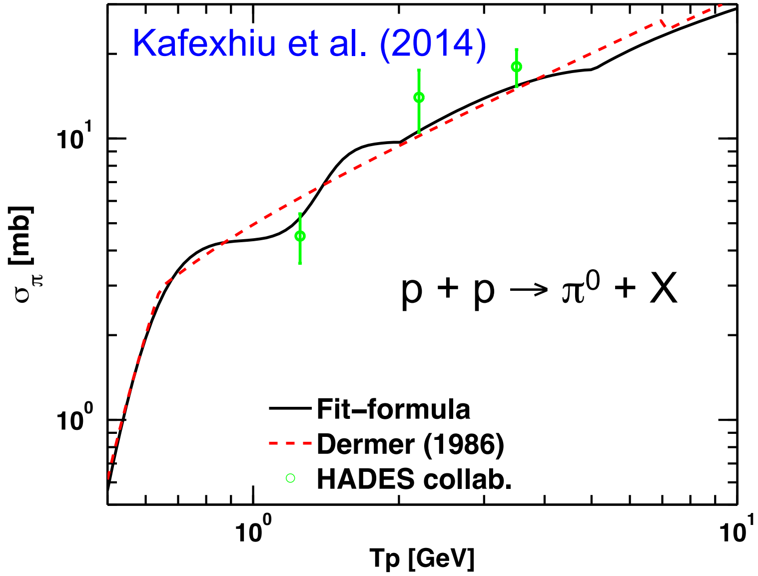

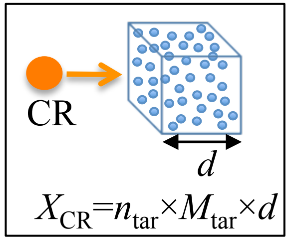

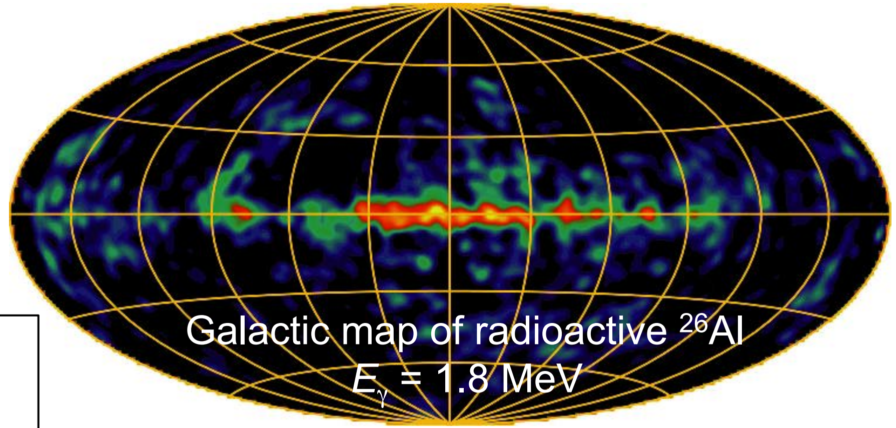

- **Kinetic power of cosmic rays** injected in the Galaxy and producing the diffuse gamma-ray emission:

$$L_{CR} = L_\gamma / R_\gamma \sim 10^{41}\ \text{erg/s},$$

where $R_\gamma \sim 0.004$ is the γ-ray radiation yield (= efficiency) for $p + p \rightarrow \pi^0 + X$

See below

$$R_\gamma \sim \frac{E_\pi N_\pi}{\langle E_{CR} \rangle} \sim \frac{m_\pi c^2}{\langle E_{CR} \rangle} \frac{X_{CR}}{m_p} \sigma_{pp\rightarrow\pi^0} \sim \frac{135\ \text{MeV}}{1\ \text{GeV}} \frac{10\ \text{g/cm}^2}{1.7\times10^{-24}\ \text{g}} \times 5\ \text{mb}$$

Strong et al. (2010): $L_{CR}(0.1 - 100\ \text{GeV})$: $(6 - 8)\times10^{40}$ erg/s

- Present-day mass of ^{26}Al ($\tau \approx 10^6$ yr) in the Galaxy: $2.8 \pm 0.8\ M_{sol}$ (Diehl+ 2006)

⇒ ~ **2 SN per century**

- Total kin. power supplied by SNe: 1.5×10^{51} erg per SN × 50 yr^{-1} ≈ **10^{42} erg s^{-1}**

⇒ Required acceleration efficiency per SN to produce the GCR: **~10%**

1. Diffusive shock acceleration in SN shocks

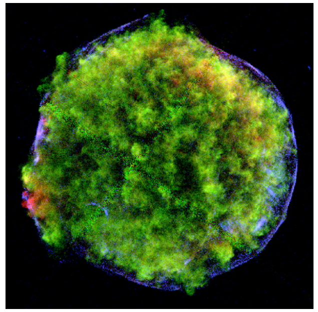

- High-velocity ejecta in supernova explosion: ~ 10 000 km/s
- **Strong shock**, with initial sonic Mach number $M_S = V_s / c_S > 100$ with the sound speed $c_S \approx 100\ (T/10^6\ \mathrm{K})^{0.5}$ km/s
- First-order Fermi (1949) acceleration process in SN shock waves (Krymskii 1977; Bell 1978; Axford et al. 1978; Blandford & Ostriker 1978)
- Particle diffusion on magnetized turbulence on both sides of the SN shock

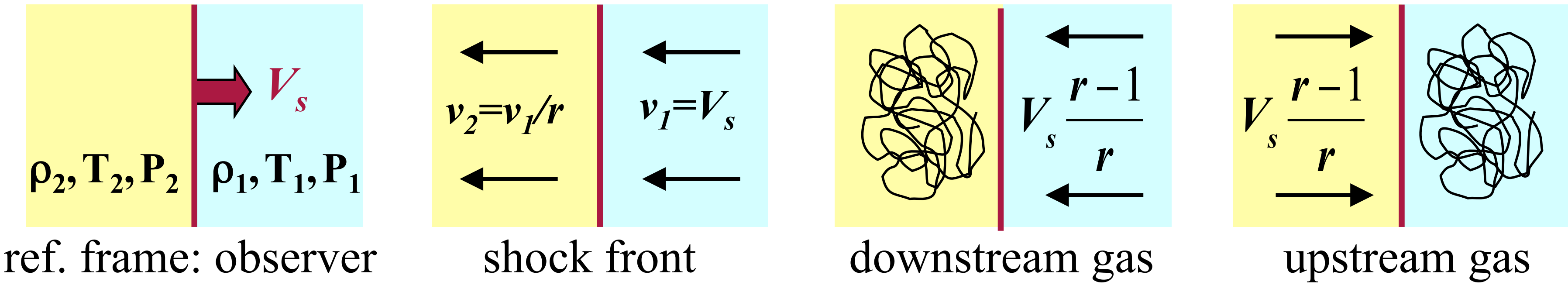

- Fractional momentum gain after each cycle up-down-up: $\frac{\Delta p}{p} = \frac{4}{3}\frac{r-1}{r}\frac{V_s}{v} = \beta_{\mathrm{acc}}$
- Particle momentum spectrum: $\mathrm{d}N/\mathrm{d}p(p) \propto p^{-q}$ with $q = (r + 2) / (r - 1)$
  (for a test-particle strong shock $r = 4 \Rightarrow q = 2$)

1. Maximum cosmic-ray energy in a SNR

- **Hillas criterion**: the maximum energy a particle can achieve is such that its Larmor radius $R_L = p/ZeB$ is equal to the accelerator size R (confinement)

$$\Rightarrow \quad E_{max} = 46Z\left(\frac{B}{5\ \mu G}\right)\left(\frac{R}{10\ \mathrm{pc}}\right)\ \mathrm{PeV}$$

- From the **rate of energy gain by diffusive shock acceleration** and the **finite age of the SNR shock** (Lagage & Cesarsky 1983): $\boldsymbol{E_{max} < 30\ Z\ B_{\mu G}}$ **TeV**

$\Rightarrow$ E_{max} can reach the knee of the CR spectrum if the magnetic field in the acceleration region is **amplified to $\boldsymbol{B \sim 100\ \mu G}$** (Fe to the ankle: $\boldsymbol{B \sim 5}$ **mG**)

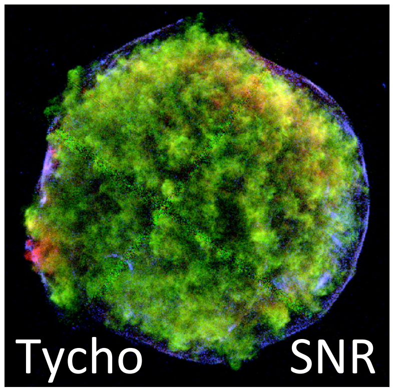

MHD simulation showing the generation of magnetic turbulence by the cosmic-ray streaming instabilities (Bell et al. 2014)

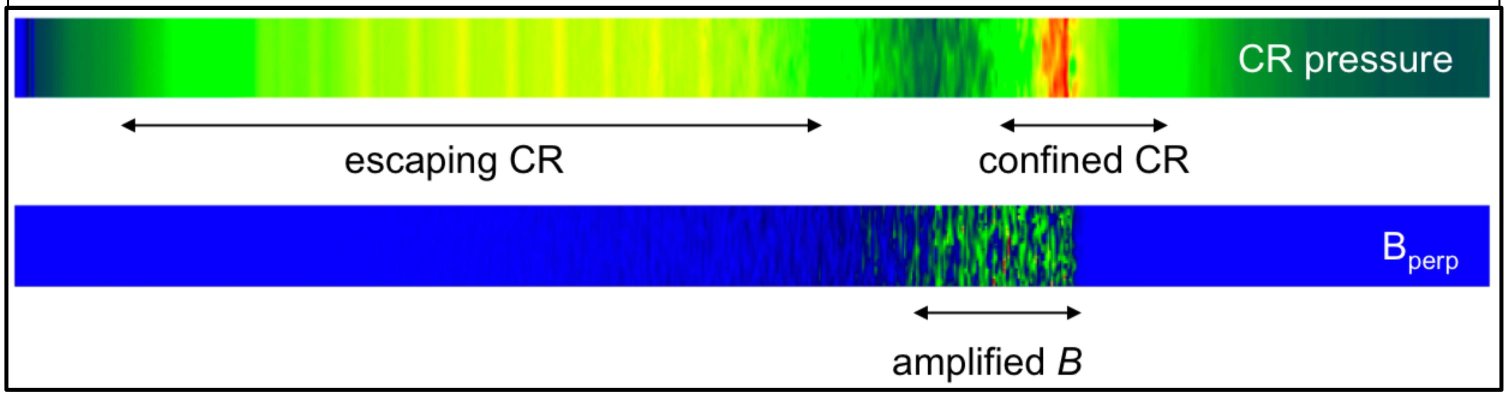

2. Supernovas and supernova remnants

2. Supernova Types

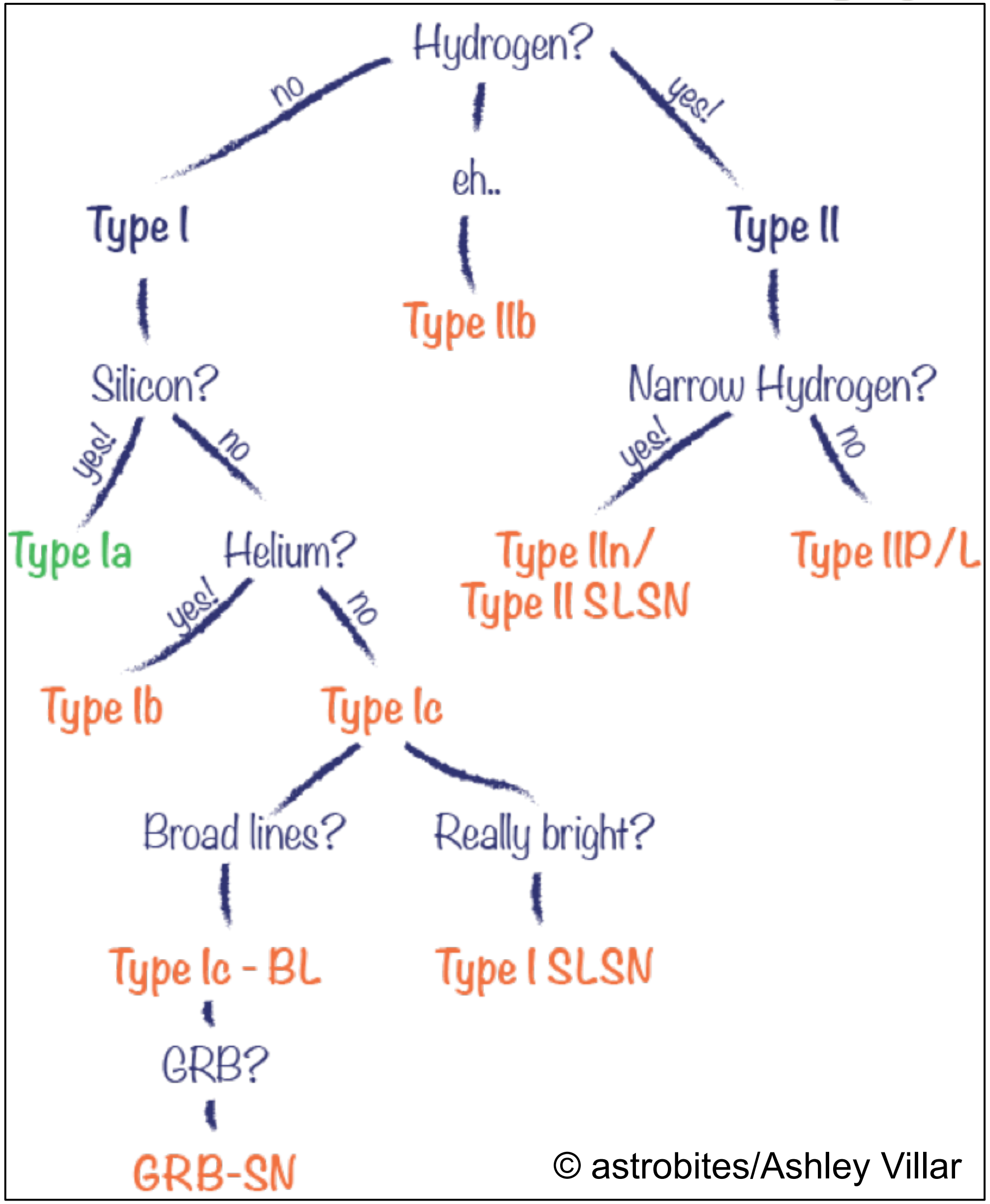

- **Type Ia supernova** (27%): explosion of a (CO) white dwarf in a binary system (WD + Main Sequence or WD+WD)

- **Type IIP supernova** (43%): explosion of a **red supergiant star** of initial mass between 8 and 16.5 M_{sol} (no strong wind)
- **Type Ib/Ic supernova** (22%): explosion of a **Wolf-Rayet star**

- SN frequency: Smartt et al. (2009)

2. SNR evolution - free expansion phase

- Power-law density profile of the **outer SN ejecta**: $\rho_{ej} = C_2\, t^{\,n-3}\, R^{-n}$, with $8 < n < 12$ (Matzner & McKee 1999)
- Circumstellar medium (CSM): $\rho_{CSM} = C_1\, R^{-s}$ with $s = 0$ for a uniform ISM or $s = 2$ for a standard wind density profile

⇒ **The forward shock position** and **shock structure** during the initial **free expansion** phase can be described by a **self-similar analytical model** (Chevalier 1982): $R_s \propto t^m$, with $m = (n\text{-}3)\,/\,(n\text{-}s)$ (deceleration para.)

- Depends on the adiabatic index of the shocked gas (PV^{γ}=cst), $\gamma = 5/3$ $(4/3)$ for an ideal non-relativistic (relativistic) gas
- Model consistent with radio observations ($0.3 < \nu < 115$ GHz) of extragalactic SNe: synchrotron emission from the shock region

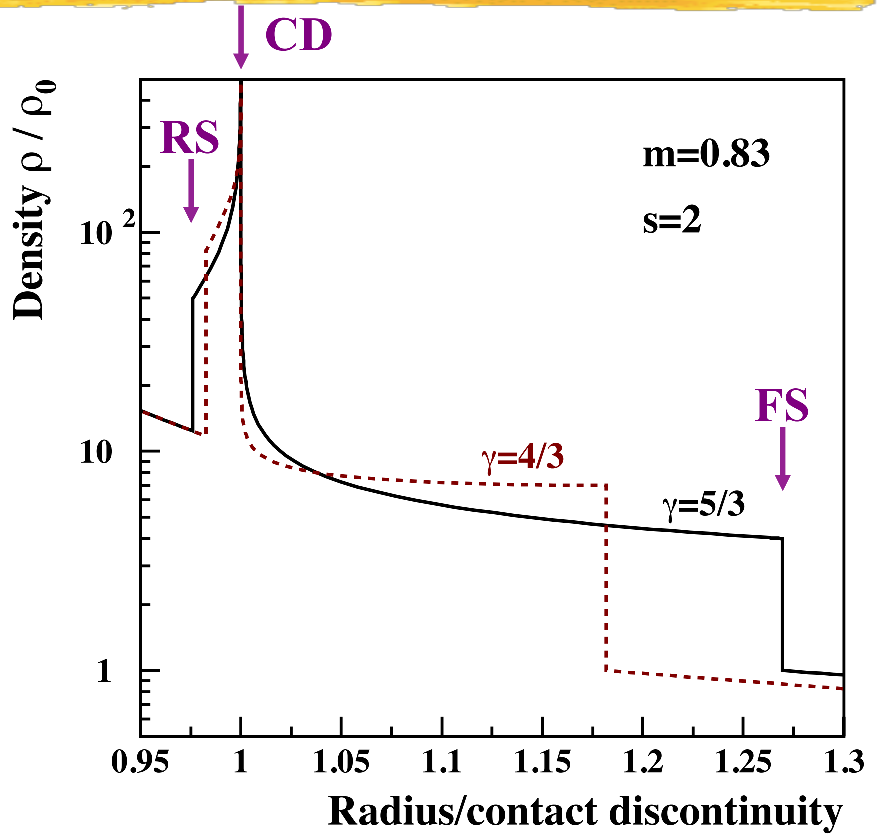

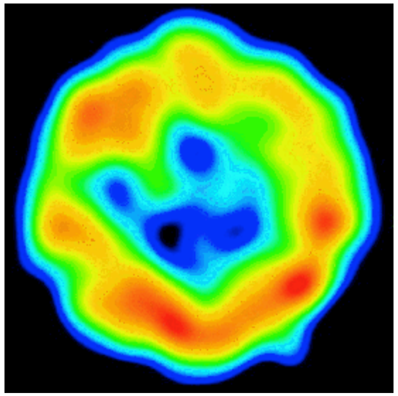

Very-long-baseline interferometry (VLBI) radio image of **SN 1993J**, day 2787 after outburst (Bartel et al. 2007)

2. Extragalactic radio supernovae

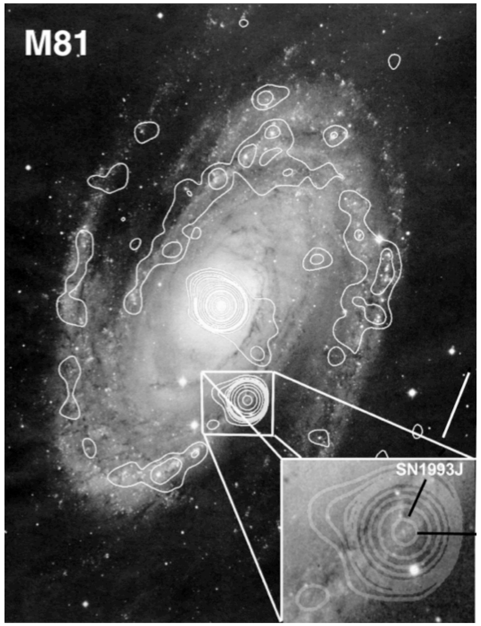

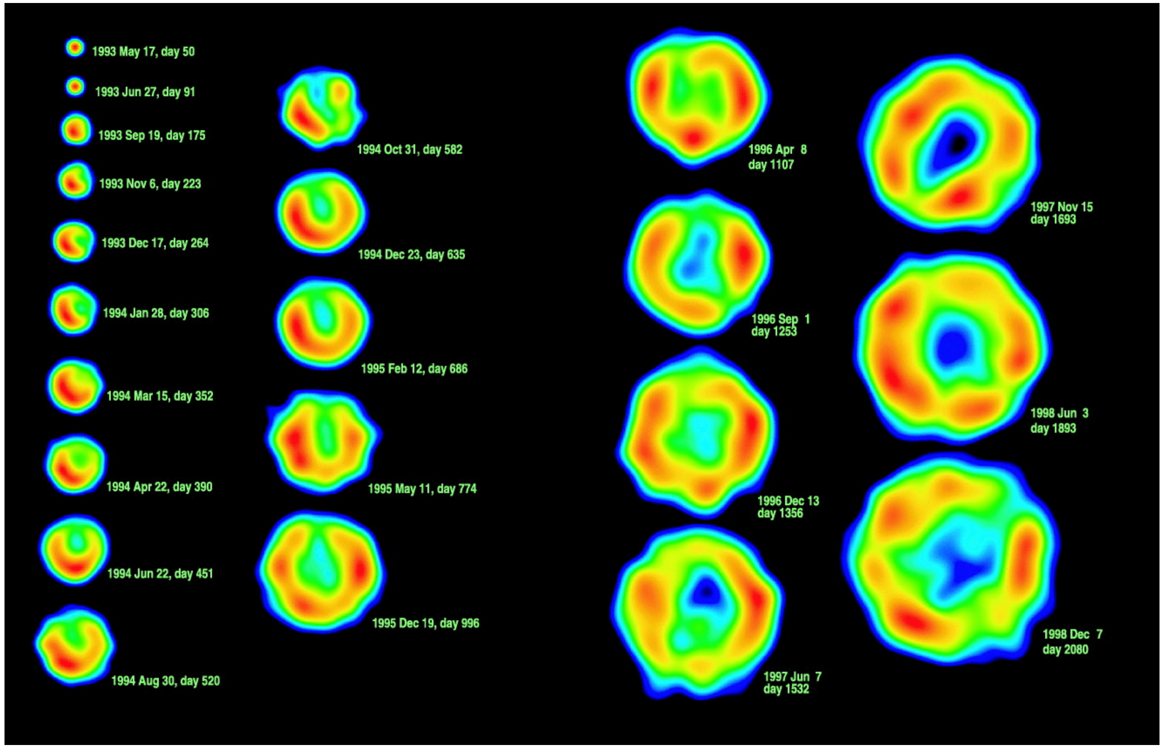

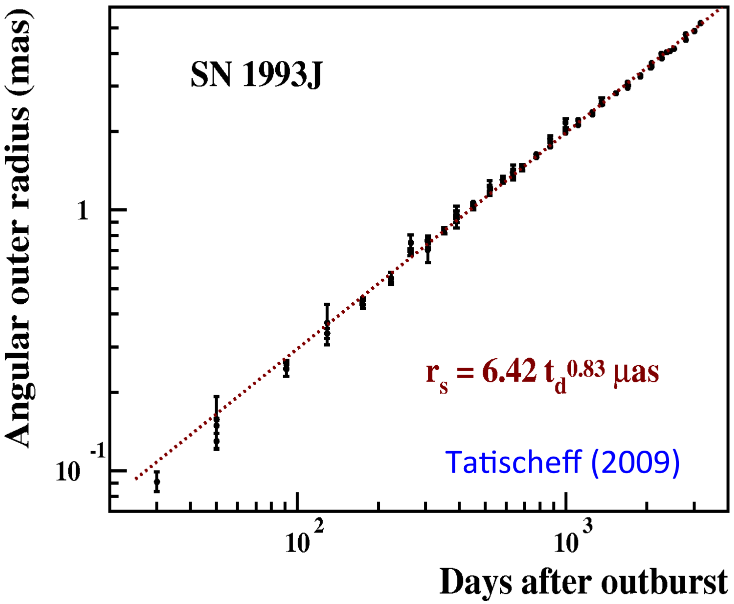

- SN 1993J: Type IIb, discovered on 1993 March 28 in the galaxy M81 (D=3.63 ± 0.34 Mpc)
- Electron DSA (?) started at t_0 < ~1 day
- Measured deceleration parameter $m = 0.83$, consistent with $s = 2$ (red supergiant wind) and $n \sim 8$ (OK with SN model, e.g. Arnett 1988)

2. SNR evolution - Sedov & radiative phases

- End of free expansion when the swept-up mass becomes comparable to the SN ejecta mass, which occurs at the time (Truelove & McKee 1999):

$$t_{\rm ST} \approx (1400~{\rm yr}) \left(\frac{M_{\rm ej}}{10~M_\odot}\right)^{5/6} \left(\frac{E_{\rm SN}}{10^{51}~{\rm erg}}\right)^{-1/2} \left(\frac{n_{\rm H}}{1~{\rm cm}^{-3}}\right)^{-1/3}$$

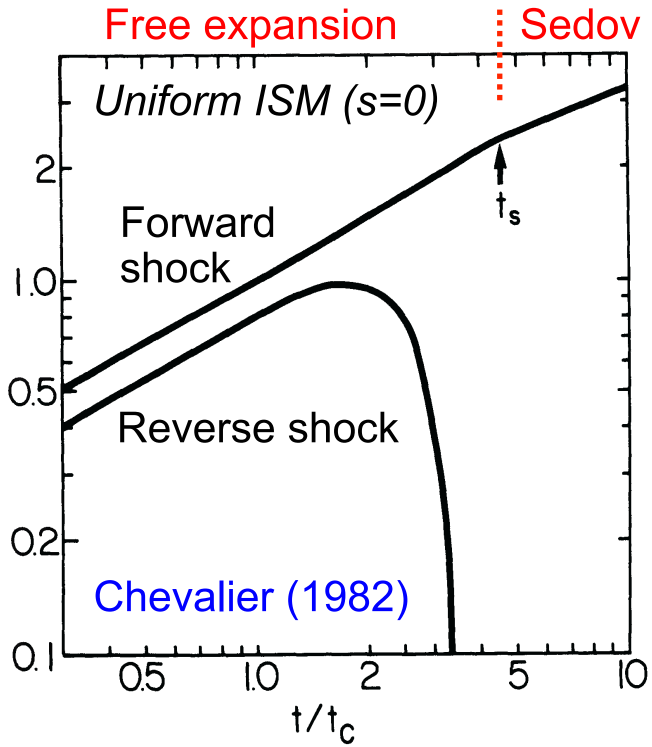

- In the subsequent adiabatic, **Sedov-Taylor phase**, the flow tends toward the **self-similar solution** for a point explosion in a power-law density profile medium (Sedov 1959), with (for a uniform ISM with $s = 0$):

$$R_s = (12.5~{\rm pc}) \left(\frac{E_{\rm SN}}{10^{51}~{\rm erg}}\right)^{1/5} \left(\frac{n_{\rm H}}{1~{\rm cm}^{-3}}\right)^{-1/5} \left(\frac{t}{10^4~{\rm yr}}\right)^{2/5}$$

- Transition to the **radiative-pressure-driven snow-plow** phase at (Blondin et al. 1998)

$$t_{\rm rad} \approx (2.9 \times 10^4~{\rm yr}) \left(\frac{E_{\rm SN}}{10^{51}~{\rm erg}}\right)^{4/17} \left(\frac{n_{\rm H}}{1~{\rm cm}^{-3}}\right)^{-9/17}$$

- In the radiative phase: recombination of the swept-up gas $\Rightarrow$ progressive cessation of the acceleration process $\Rightarrow$ escape of the CRs into the ISM

2. SN expansion into a circumstellar wind

- Assuming that a constant fraction of the blast wave mechanical power goes into CR particles:

$$\dot{W}_{\rm CR} = f_{\rm CR}\dot{W}_s = f_{\rm CR} \times \frac{1}{2}\rho_{\rm CSM}V_s^3 \times 4\pi R_s^2$$

⇒ For $s = 2$ (wind): $\dot{W}_{\rm CR} \propto t^m$, with $-0.5 < m < -0.3$

⇒ $\dot{W}_{\rm CR}$ is maximum just after the outburst

- High $\rho_{\rm CSM}$ and V_s ⇒ high amplified B ($B^2/8\pi \propto \rho_{\rm CSM}V_s^2$) ⇒ high E_{max} (Völk & Biermann 1988)
- SN IIb: explosion of a red supergiant in a dense wind, ~5% of core-collapse SNe (Smartt et al. 2009)

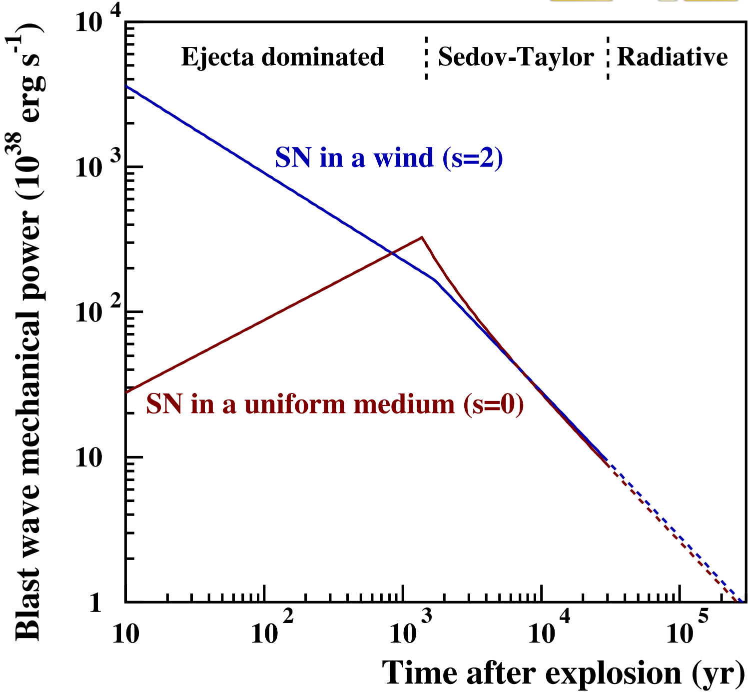

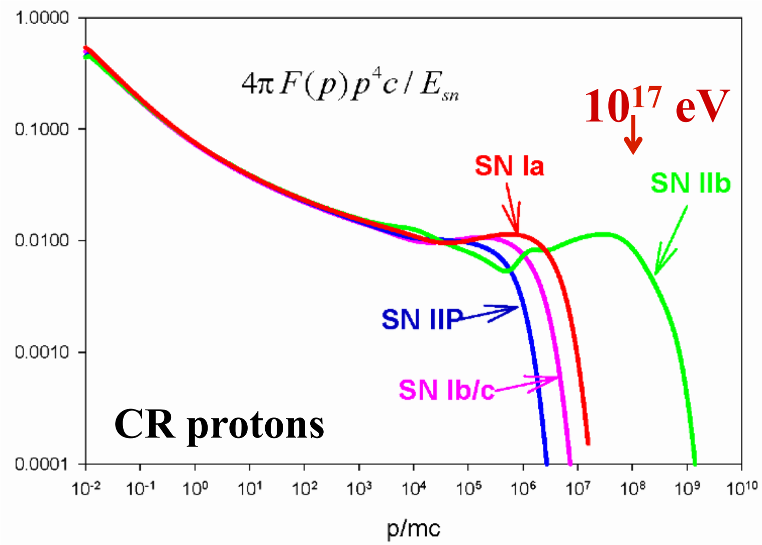

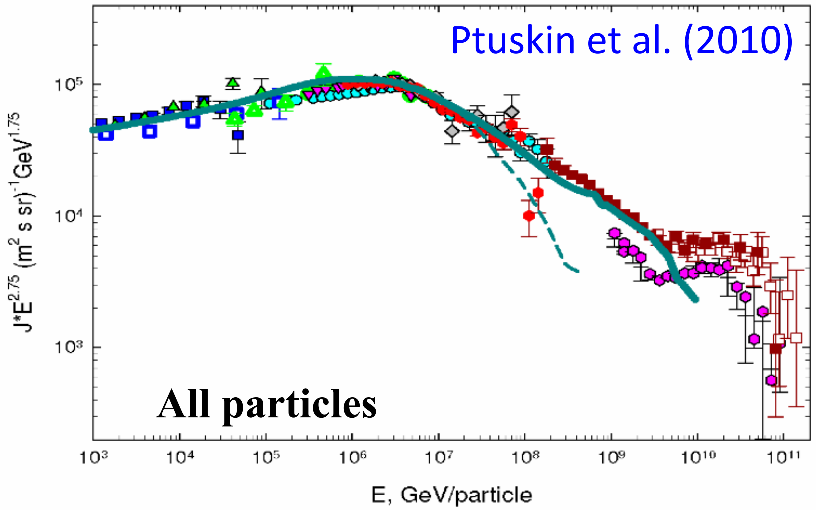

2. Cosmic-ray modified shock

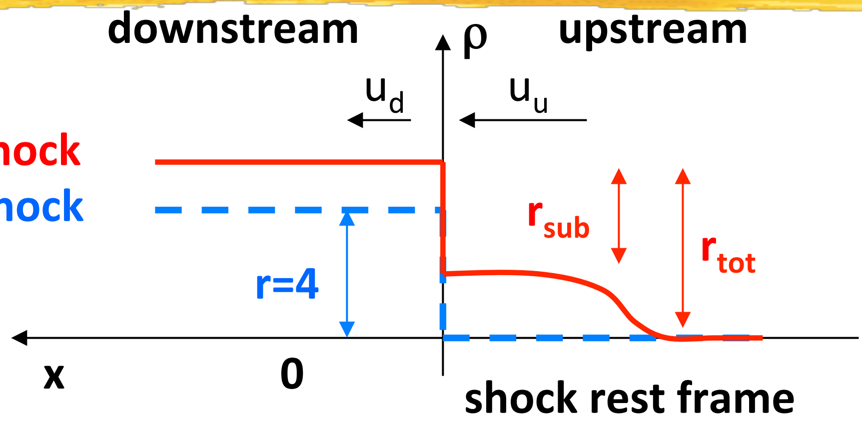

Conservation equations:

- $\rho_0 u_0 = \rho(x) u(x)$ (mass flux)
- $\rho_0 u_0^2 + P_{g,0} = \rho(x) u(x)^2 + P_g(x) + \boldsymbol{P_{CR}(x)}$ (momentum flux)
- $\frac{1}{2}\rho_0 u_0^3 + \frac{\gamma_g}{\gamma_g - 1} P_{g,0} u_0 - F_E = \frac{1}{2}\rho(x) u(x)^3 + \frac{\gamma_g}{\gamma_g - 1} P_g(x) u(x) + \frac{\gamma_c}{\gamma_c - 1} P_{CR}(x) u(x)$

escaping energy flux (energy flux)

with $P_{CR}(x) = \frac{1}{3}\int_{p_{\rm inj}}^{p_{\max}} dp\, 4\pi p^3 v(p) f(x,p)$

particle distribution function

Diffusive transport equation:

- $\frac{\partial}{\partial x}\left[D(x,p)\frac{\partial}{\partial x} f(x,p)\right] - u\frac{\partial f(x,p)}{\partial x} + \frac{1}{3}\left(\frac{\mathrm{d}u}{\mathrm{d}x}\right) p \frac{\partial f(x,p)}{\partial p} + Q(x,p) = 0$

2. Estimate of the DSA efficiency

Hydrodynamic simulations
(Ferrand et al. 2012)

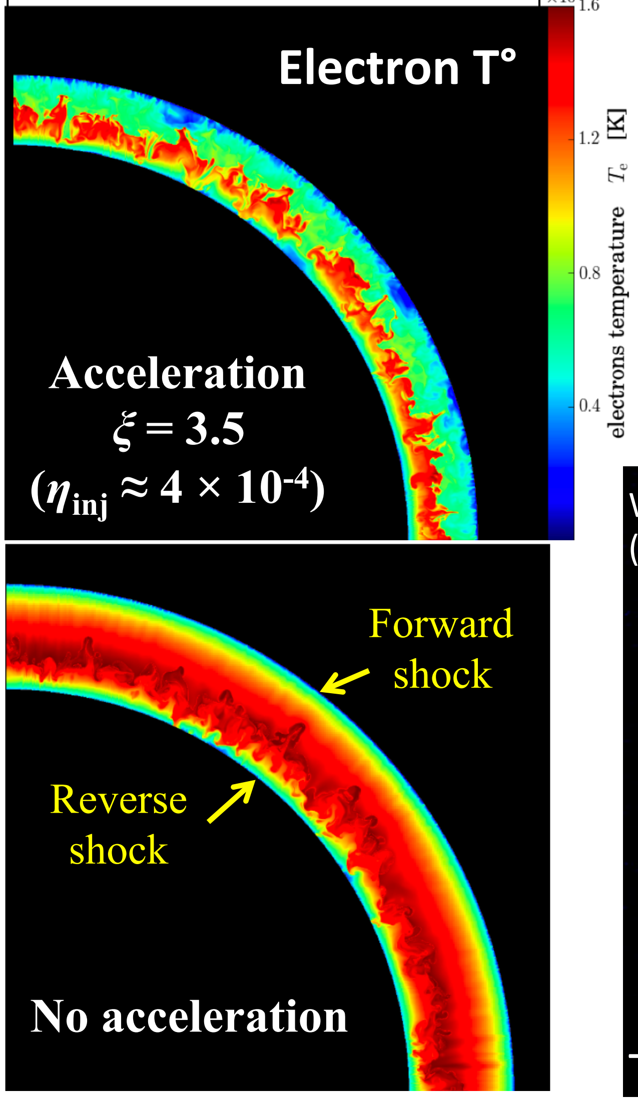

- Efficient acceleration of hadronic CRs in SNRs impacts:
  - the **remnant morphology** (e.g. Warren et al. 2005)
  - the **post-shock temperature** (e.g. Helder et al. 2009)
  - the **amplified B-field** (e.g. Eriksen et al. 2011)
  - the **gamma-ray emission** (e.g. Acero et al. 2016)

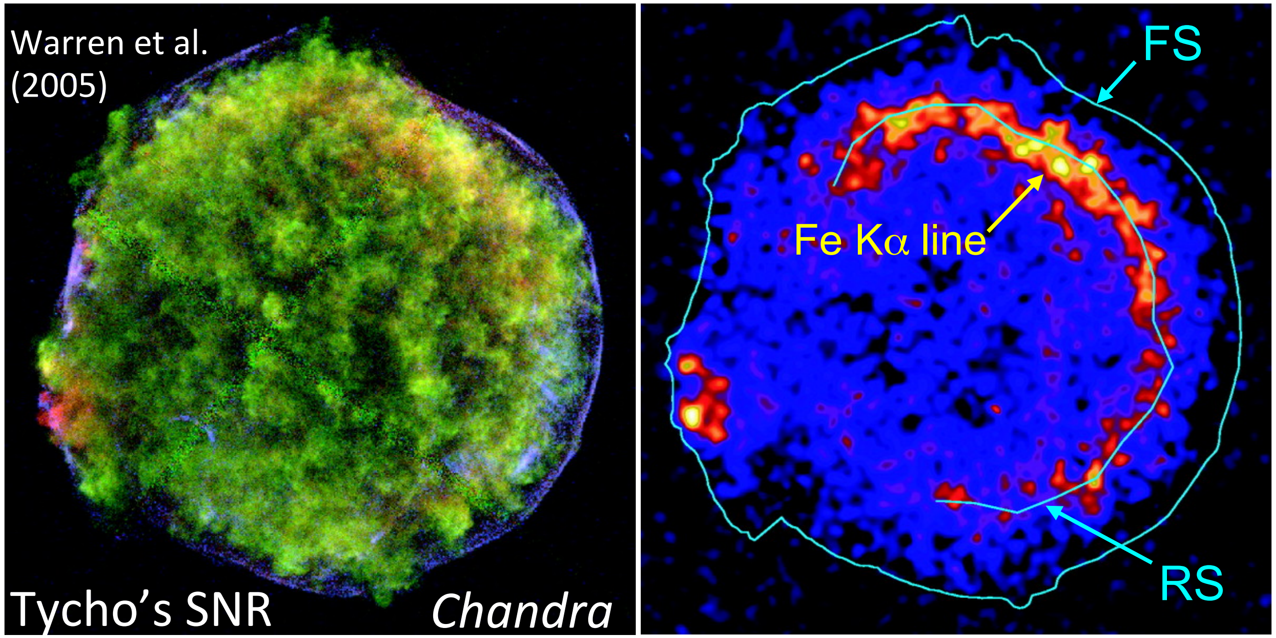

2. Post-shock temperature

- In a test-particle (no CR) strong shock: $kT_2 = \frac{P_2}{\rho_2}\mu m_{\mathrm{H}} = \frac{3\rho_1 V_s^2}{4}\frac{\mu m_{\mathrm{H}}}{4\rho_1} = \frac{3}{16}\mu m_{\mathrm{H}} V_s^2$
  (μm_{H} is the mean particle mass)
- But in a CR-modified shock with $P_2 = P_g + P_{\mathrm{CR}}$, $\boldsymbol{T_2}$ **can be much lower** (for a given V_s)
- Low T_e found in SNR 1E 0102-72 (*Chandra*; Hughes et al. 2000), but T_e - T_i equilibration?
- **Balmer Hα line** (n=3→2) profile: narrow component from excitation of H atoms upstream + **broad component** from charge transfer dowstream => **T° of the post-shock protons**

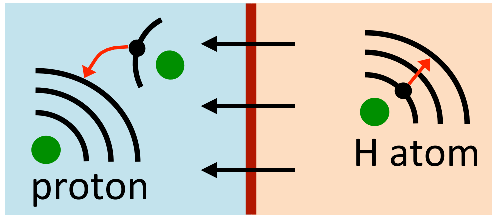

- In RCW 86, **>50%** of the post-shock pressure is **due to CRs** (Helder et al. 2009)

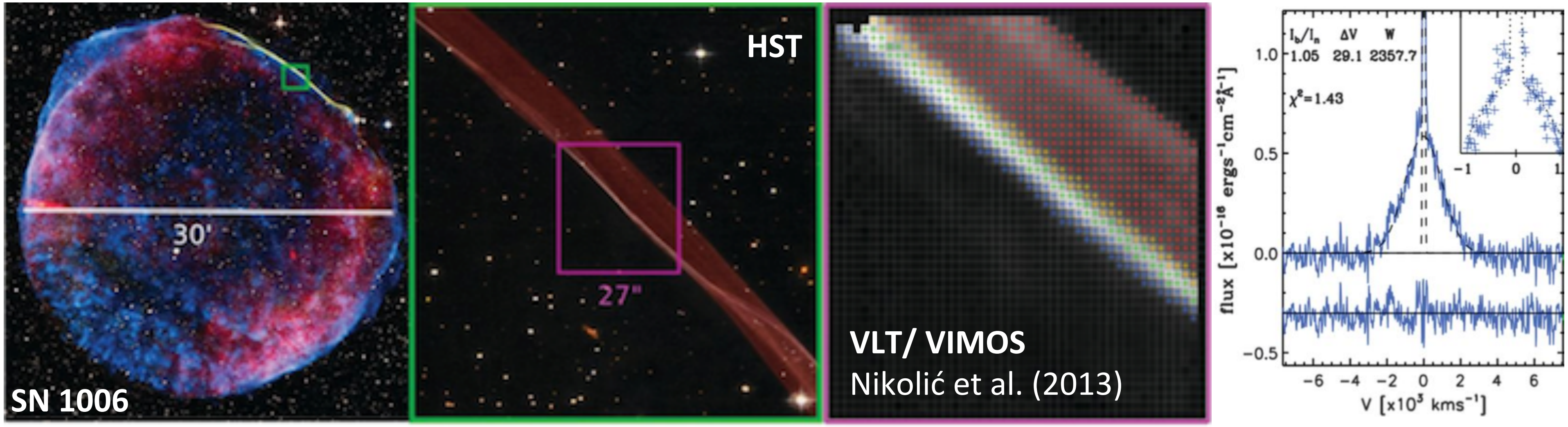

2. Evidence for B-field amplification

- Postshock magnetic field estimated from synchrotron X-ray filaments (e.g. Vink & Laming 2003; Parizot et al. 2006) and variability of X-ray bright spots (e.g. Uchiyama et al. 2007)

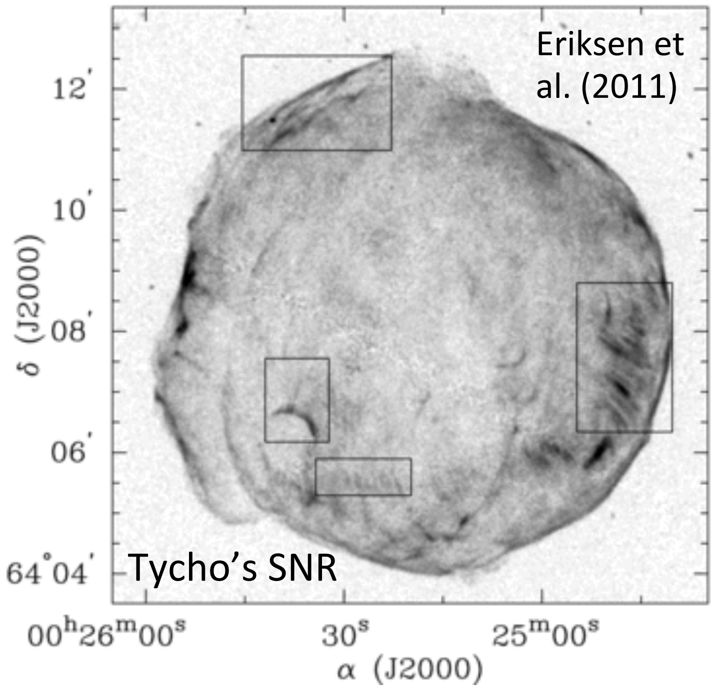

- Width of synchrotron filaments $l_{\rm syn} \sim l_{\rm adv} = t_{\rm syn}\, V_s/r$ where the synchrotron loss time $t_{\rm syn} \propto E_e^{-1}\, B^{-2}$
- Given the relation between the synchrotron photon energy $E_{\rm syn}$, the electron energy E_e and B, $E_{\rm syn} \approx 40\ {\rm keV} \times (B\ /\ 100\ \mu{\rm G}) \times (E_e\ /\ 100\ {\rm TeV})^2$:

$$l_{\rm adv} = 1.4\times10^{17}\left(\frac{B}{100\ \mu{\rm G}}\right)^{-3/2}\left(\frac{E_{\rm syn}}{5\ {\rm keV}}\right)^{-1/2}\left(\frac{V_s}{5000\ {\rm km/s}}\right)\left(\frac{r}{4}\right)^{-1}\ {\rm cm}$$

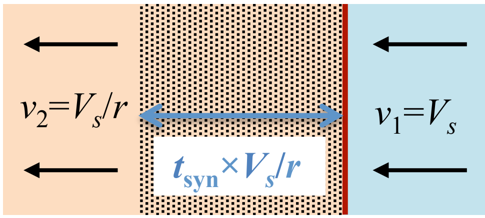

- In Tycho/SN 1572, $l_{\rm syn} \approx 1.6'' \approx 5\times10^{16}$ cm ($D \approx 2$ kpc) $\Rightarrow$ $\boldsymbol{B \sim 200\ \mu{\rm G}}$, much higher that the compressed interstellar field $B \sim 3\ B_{\rm ISM} \sim 15\ \mu{\rm G}$
- B-field fluctuations excited in upstream plasma by various instabilities including **resonant** (e.g. Bell & Lucek 2001) and **non-resonant** (Bell 2004) **CR streaming instabilities**

Reville et al. (2008)

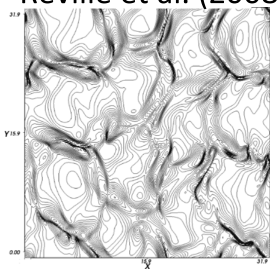

2. Gamma-ray emission of SNRs

- Gamma-ray visibility of SNRs (from pion production) predicted by Drury et al. (1994), now observed from more than 30 sources (1st *Fermi*-LAT SNR catalog; online TeVCat)

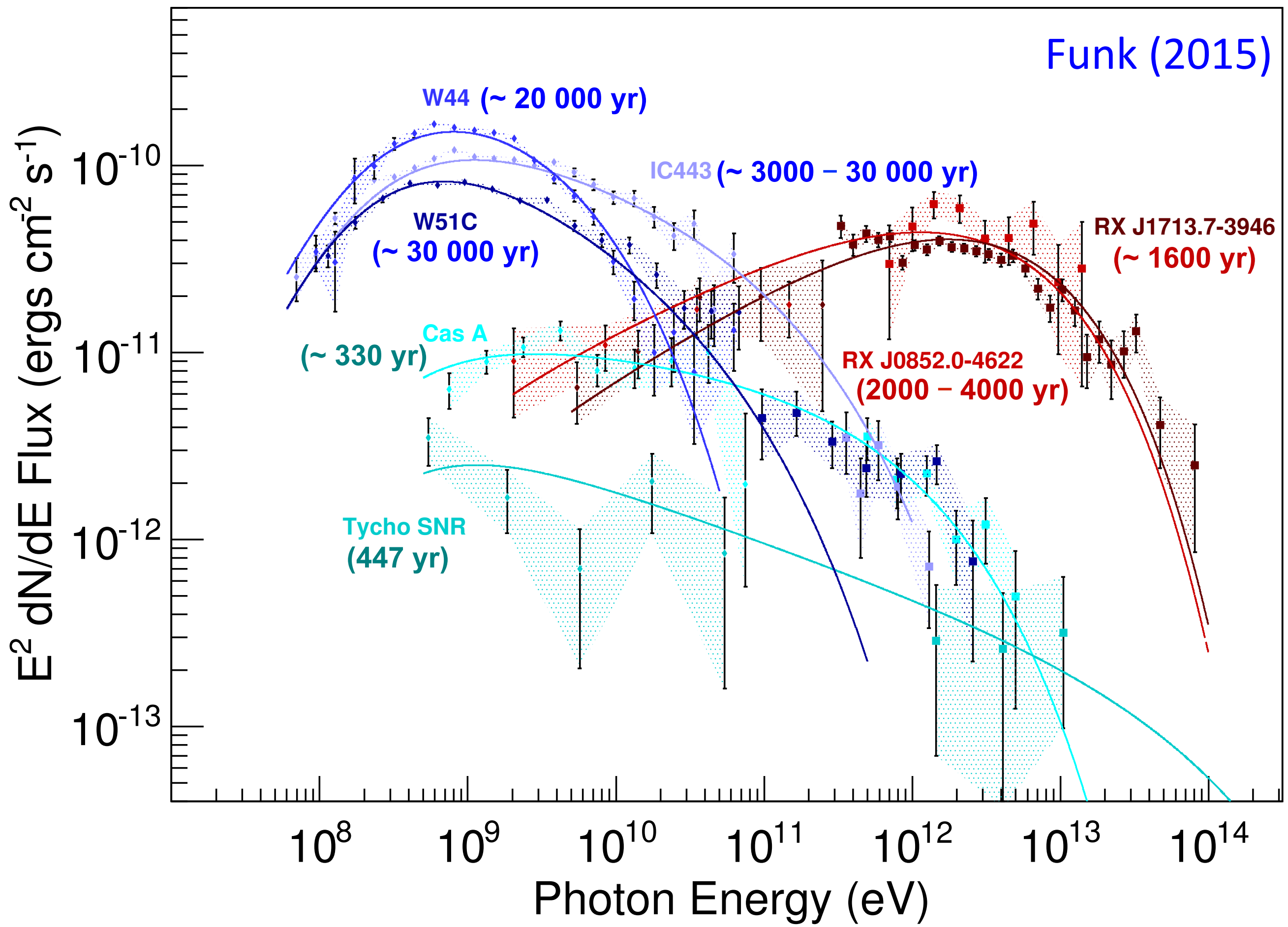

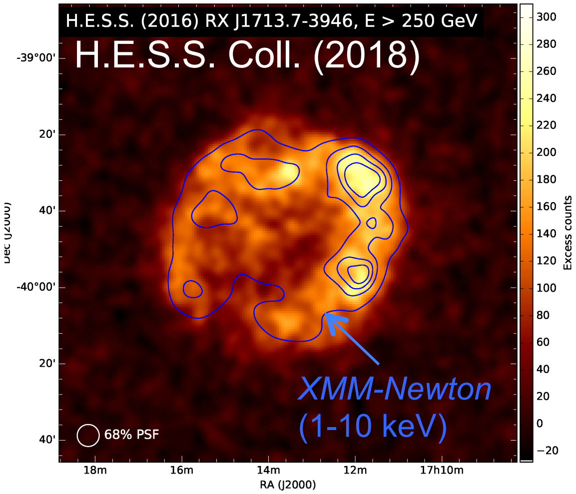

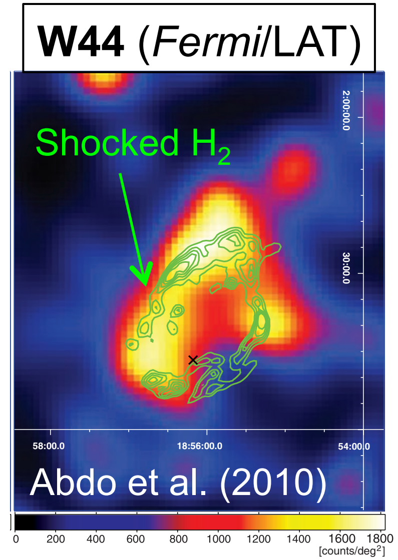

2. Gamma-ray emission of middle-aged SNRs

- Middle-aged SNRs (~ 10 - 100 kyr) **interacting with molecular clouds**
- **Hadronic γ-ray emission** (π^0 decay) from molecular clouds within the remnant and/or nearby MCs
- **Steep CR spectrum,** $q_p \approx \Gamma_{pp} \approx 2.4$ (test-particle DSA predicts $q_p = 2$)
- Origin of the GeV CRs (see Tang 2019):
  - **Fresh CRs escaping the SNR** and irradiating nearby MCs, or
  - **Pre-existing CRs compressed and re-accelerated** in **radiative shocks** slowed down by direct interaction of the SNR and a MC

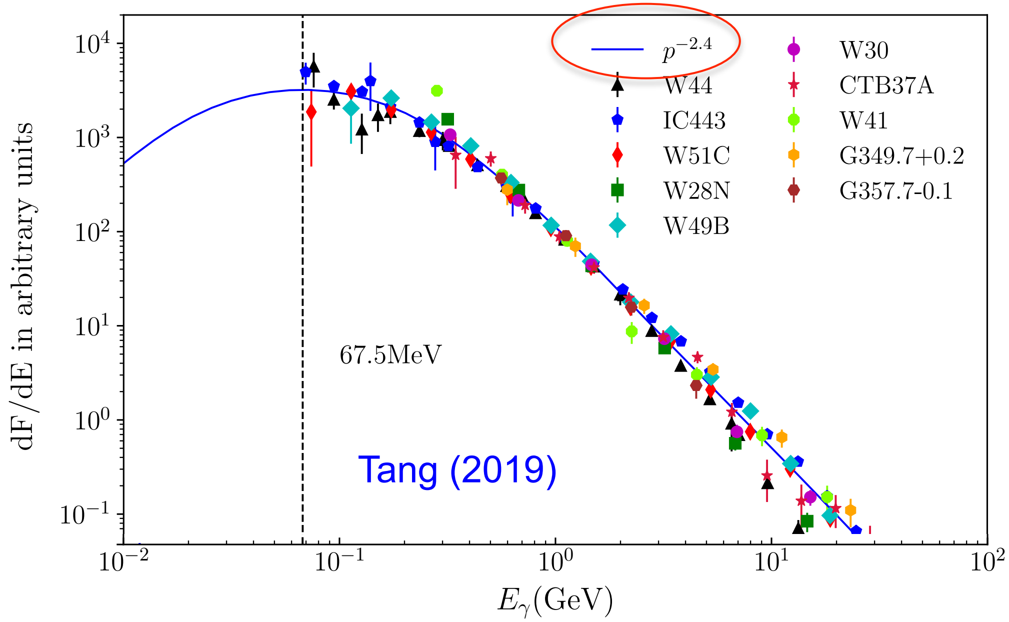

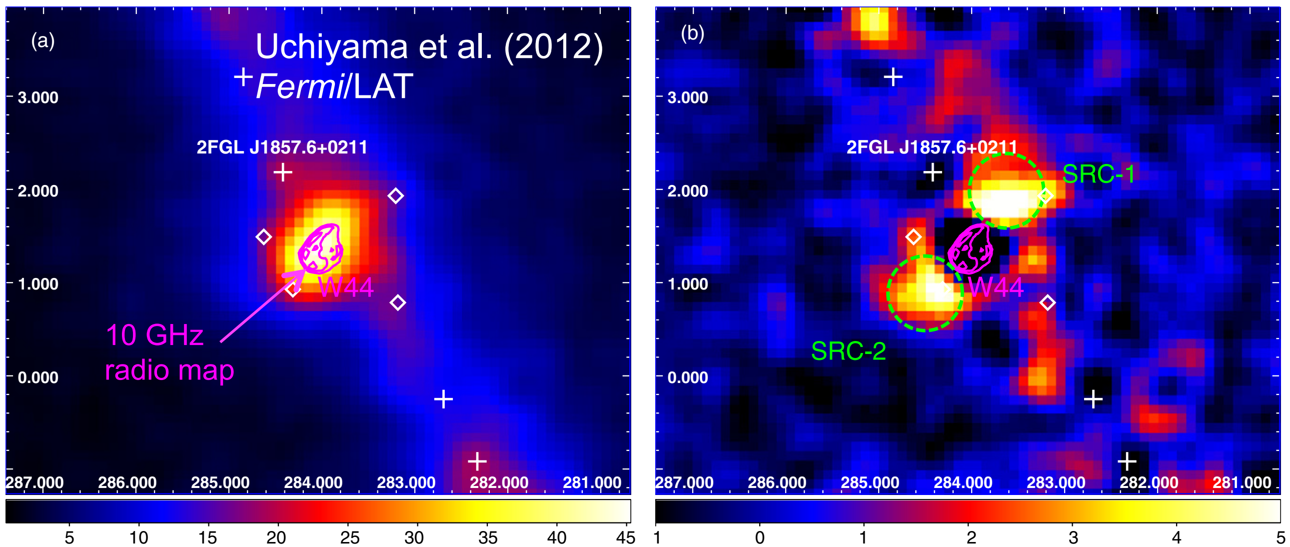

2. Gamma-ray emission of young SNRs

- In young SNRs such as **RX J1713** (CCSN; ~ 1.6 kyr), **Vela Jr** (CCSN; ~ 3 kyr), **SN 1006** (SN Ia; 1.013 kyr) and **RCW 86** (SN Ia; 1.8 kyr), the hardness of the γ-ray emission suggests a **leptonic origin from Inverse Compton scattering**: $\Gamma_{\rm IC} = (q_e+1)/2 = 1.5$ for $q_e = 2$

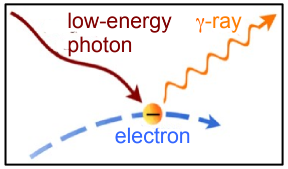

- Supported by the correlation between the TeV and X-ray (synchrotron) images

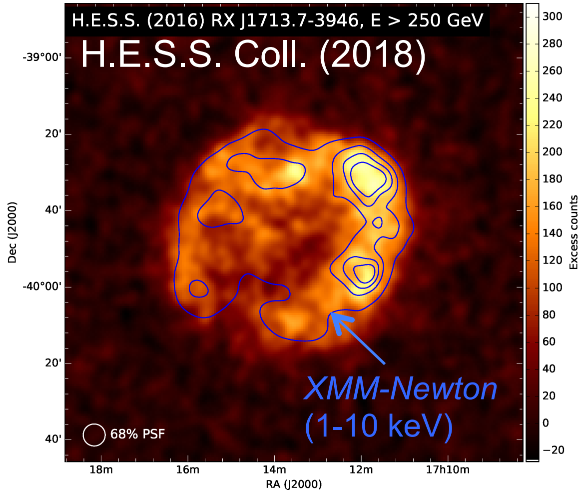

- The hadronic contribution is still debated (see Celli et al. 2019)

- In **Cas A** (**Type IIb** CCSN; ~ 330 yr) and **Tycho's SNR** (Type Ia; 447 yr), the GeV emission is **most likely hadronic** (e.g. Blasi 2014)

- TeV emission of Cas A cut-off at ~ 3.5 TeV (MAGIC) $\Rightarrow$ $E_{\rm max}({\rm p}) \sim 12$ **TeV** ($\ll 3$ PeV)

- TeV emission of Tycho cut off at ~ 2 TeV (VERITAS, Archambault et al. 2017)

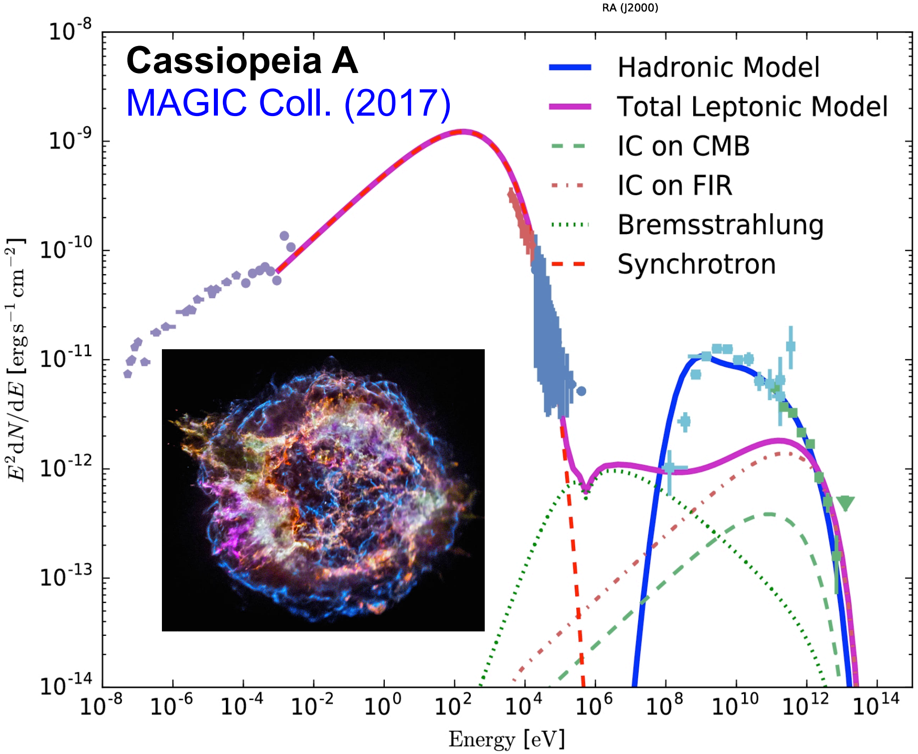

2. γ-ray emission and the SNR paradigm

- Required CR efficiency of ~ 10% per SN **compatible with 1st *Fermi*-LAT SNR catalog** (Acero et al. 2016)

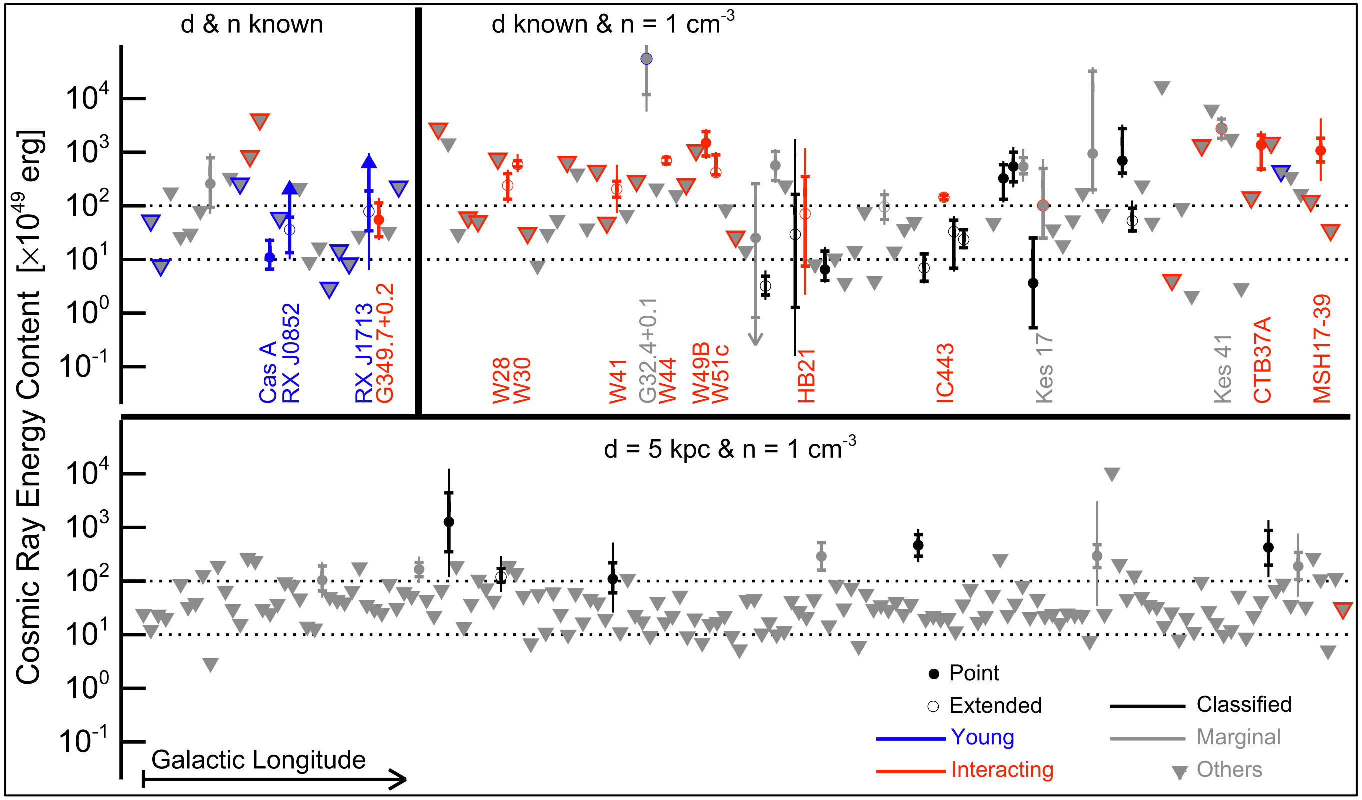

Density in the interaction region underestimated

$\varepsilon_{CR} \approx$ 10-100%

Among known radio SNRs: 30 GeV sources, 14 marginal, 245 u.l.

$\varepsilon_{CR} \approx$ 10-100%

- Predicted maximum CR proton energy (Schure & Bell 2013) vs. observations:

SNR Type	Age	R_s	u_s	$E_{max}(\gamma\tau = 5)$	B_{sat}	B_{obs}	E_{max} (obs)
RSG (Cas A)	330 yr	2.2 pc	4900 km s^{-1}	283 TeV	243 μG	210–230 μG	~12 TeV (MAGIC 2017)
Tycho	440 yr	3.2 pc	3900 km s^{-1}	108 TeV	128 μG	200–230 μG	~10 TeV (VERITAS 2017)
SN1006	1000 yr	7.6 pc	4100 km s^{-1}	<60 TeV	< 35 μG	80–150 μG	~50 TeV (Condon et al. 2016)

3. Massive star clusters and superbubbles

3. Birth of massive stars

- Massive stars are born in groups called **OB association** and their wind activities generate **superbubbles** of hot plasma, where most core-collapse SNe (~60% - ~85%) explode (Parizot et al. 2004; Higdon & Lingenfelter 2005)

- Mean **wind power per star** from a coeval population of massive stars (Voss et al. 2009): $\approx 1.5\times10^{36}$ erg/s for $\approx$ 5 - 6 Myr
  $\Rightarrow$ $\boldsymbol{E_{\rm wind} \approx (2 - 3)\times10^{50}}$ **erg**, (15 - 25)% of $E_{\rm SN}$

- **Compact star clusters** like Westerlund 1 can contain **hundreds of massive stars in a few pc^3**

- Radius of a superbubble (Weaver et al. 1977):

$$R_{\rm SB} \simeq (22{\rm pc}) t_{\rm Myr}^{3/5} N_{*,30}^{1/5} n_{\rm H,100}^{-1/5},$$

with $N_{*,30} = N_*/30$, N_* being the number of massive stars (in the mass range 8–120 $M_\odot$)

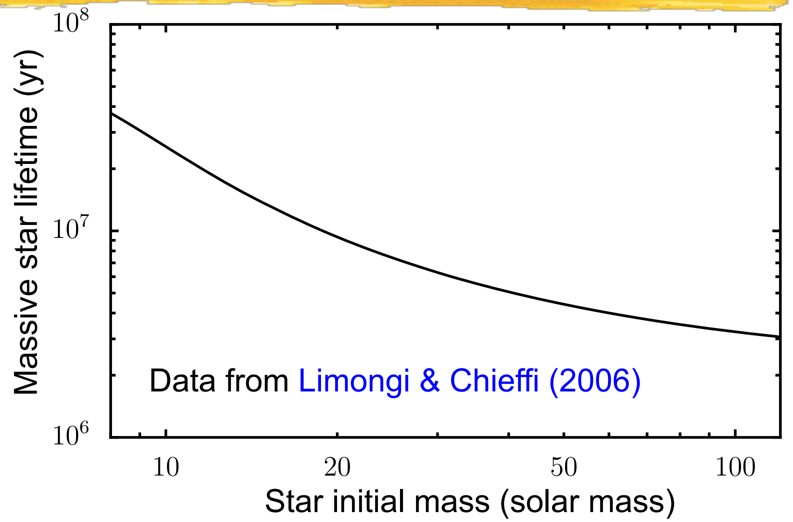

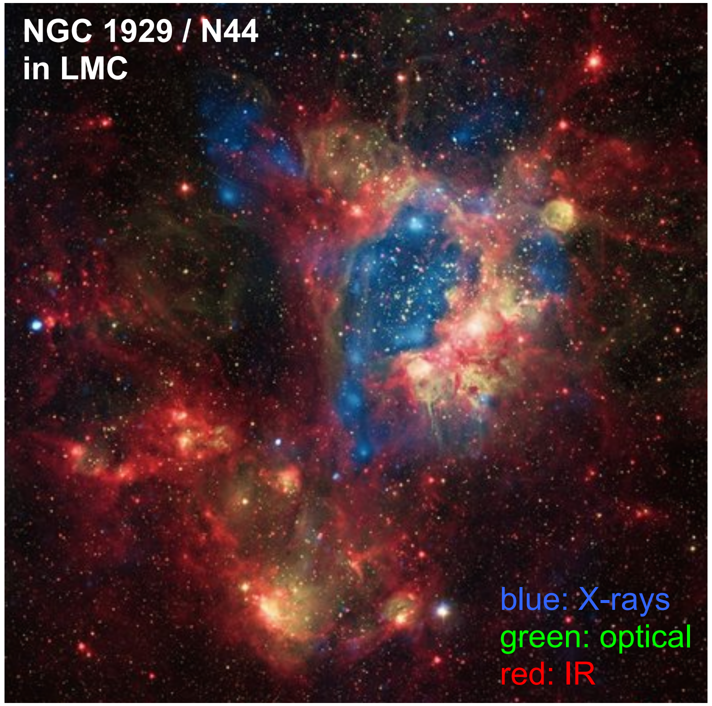

3. Acceleration in massive star clusters & superbubbles

- **Strong magnetized turbulence** generated by wind-wind and wind-clump interactions

- **Specific acceleration processes** (Bykov 2014): (i) **colliding shock flows** (wind-wind and SN-wind), (ii) turbulence (2nd order Fermi), (iii) magnetic field reconnection, (iv) multiple shocks

- Expected **hardening of the CR spectrum** due to repeated shock acceleration:
  $\mathrm{d}N/\mathrm{d}p(p) \propto p^{-q}$ with $q = 1 + P_{\mathrm{esc}} / \beta_{\mathrm{acc}}$,
  P_{esc} being the escape probability downstream
  In a single shock: $P_{\mathrm{esc}} = 4V_s/(rv) \Rightarrow q = 2$ for $r = 4$
  But if $P_{\mathrm{esc}} \rightarrow 0$ in multiple shocks: $\boldsymbol{q \rightarrow 1}$

- **Maximum CR energy can be boosted** by
  (i) turbulent B-field amplification in colliding shocks, (ii) repeated shock acceleration,
  (iii) system size ($\rightarrow$ ~100 pc; Hillas criterion)

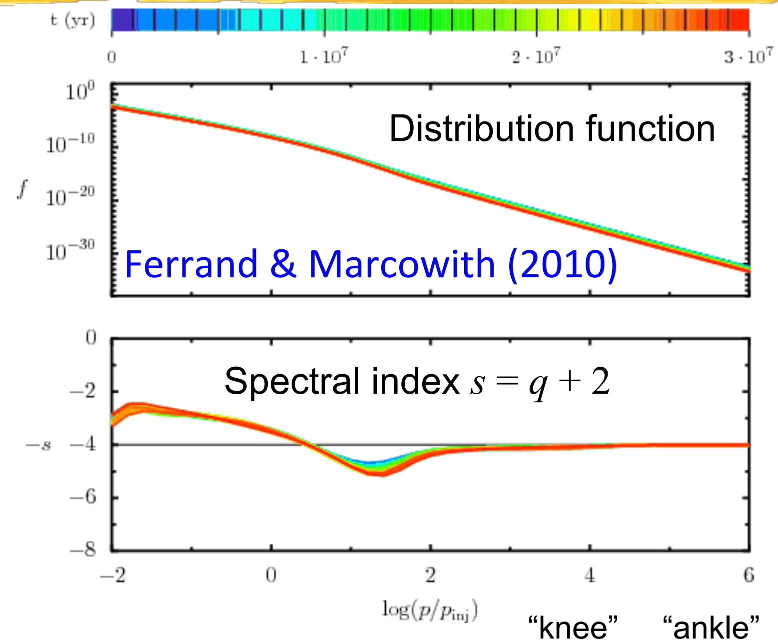

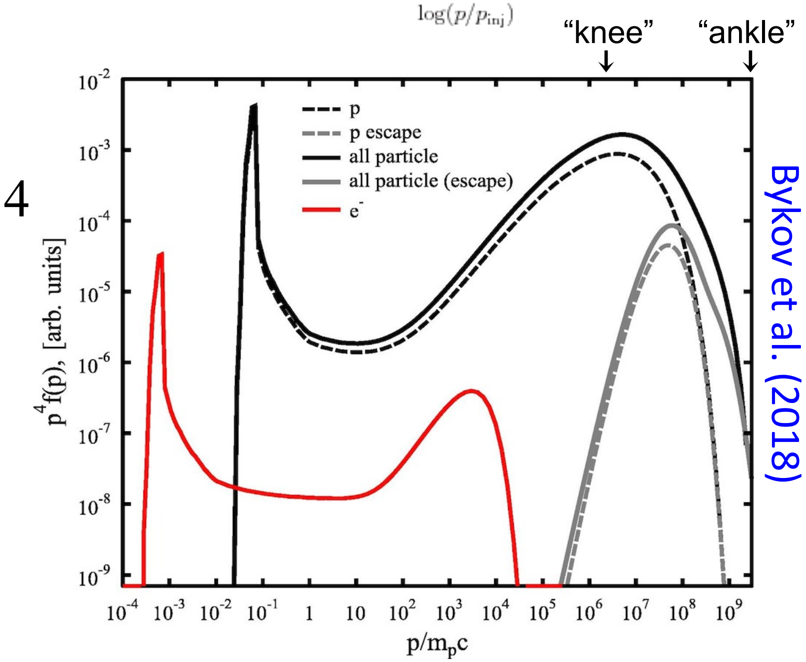

Bykov et al. (2018)

3. γ-rays from massive star clusters and superbubbles

- Diffuse GeV γ-ray emission (*Fermi*-LAT Coll. 2011) associated with the **young** massive star cluster **Cygnus OB2** (3-4 Myr; **no visible SN**): **hard spectrum** from **CRs accelerated in colliding winds** or **GCRs re-accelerated in turbulence**? (Tolksdorf et al. 2019)

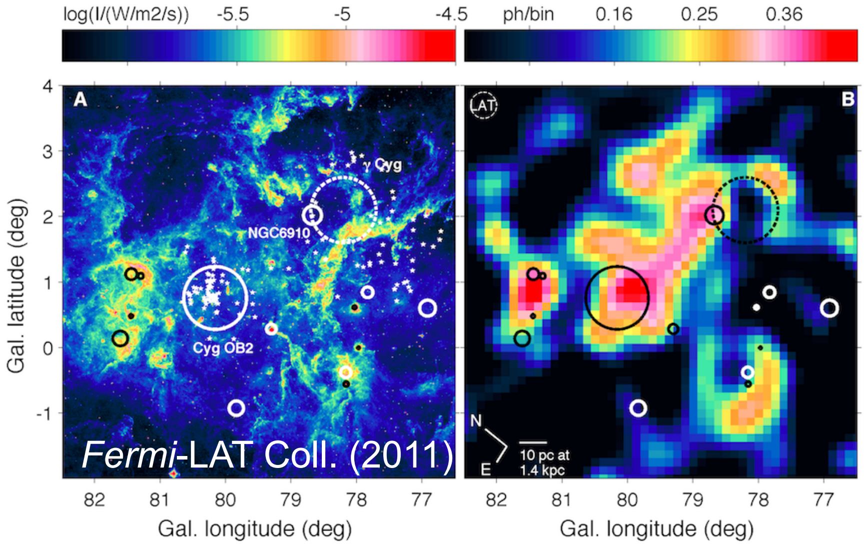

- Detection with *Fermi*-LAT of GeV γ-rays from a candidate massive OB association/ cluster **G25.18+0.26** (Katsuta et al. 2017)

- TeV γ-rays from the **superbubble 30 Doradus C** (~5 SNe) in the LMC (H.E.S.S. Coll. 2015) - Most probably leptonic (Inverse Compton) emission (Kavanagh et al. 2019)

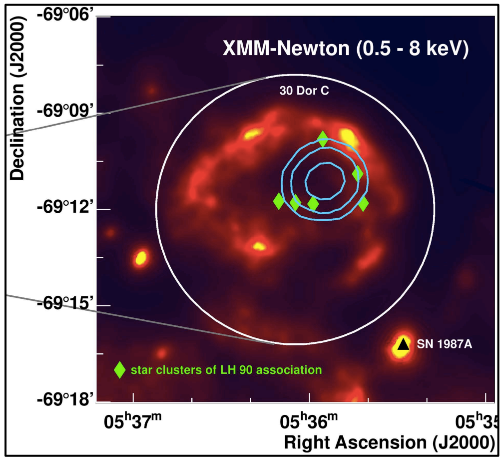

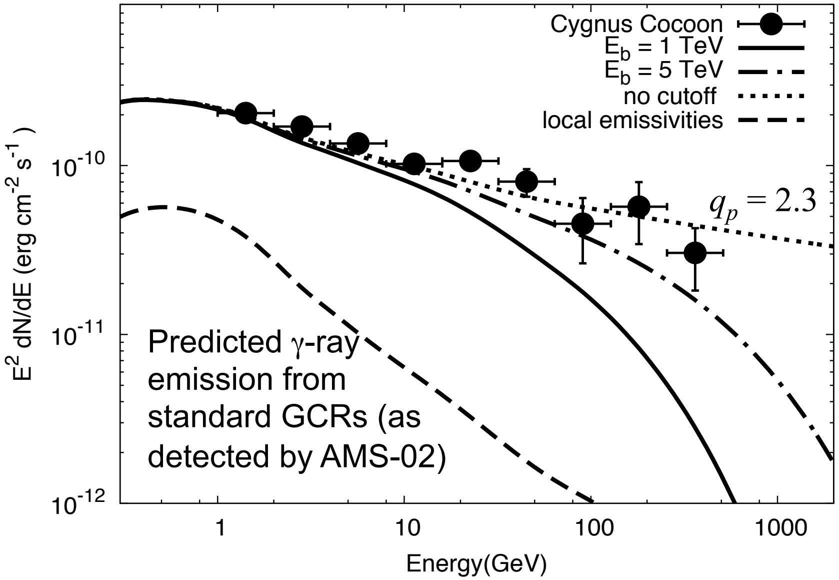

3. Galactic CRs from massive star clusters?

- Aharonian et al. (2019): Cygnus OB2 and Westerlund 1 show power-law γ-ray spectra **with no break**, similar to the TeV emission from the Central Molecular Zone (but H.E.S.S. Coll. 2018) ⇒ **massive star clusters are PeVatrons**

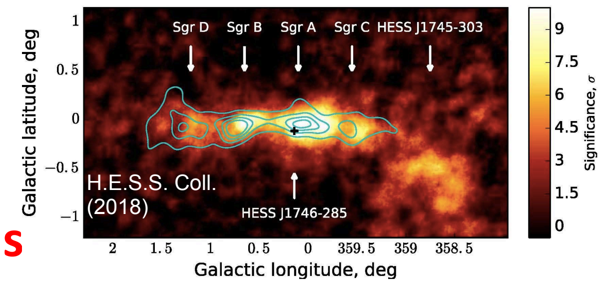

- 1/r radial distribution of CRs around the star clusters ⇒ continuous CR injection from the **stellar wind activity**, **not from intermittent SNe** (Aharonian et al. 2019)

Controversial

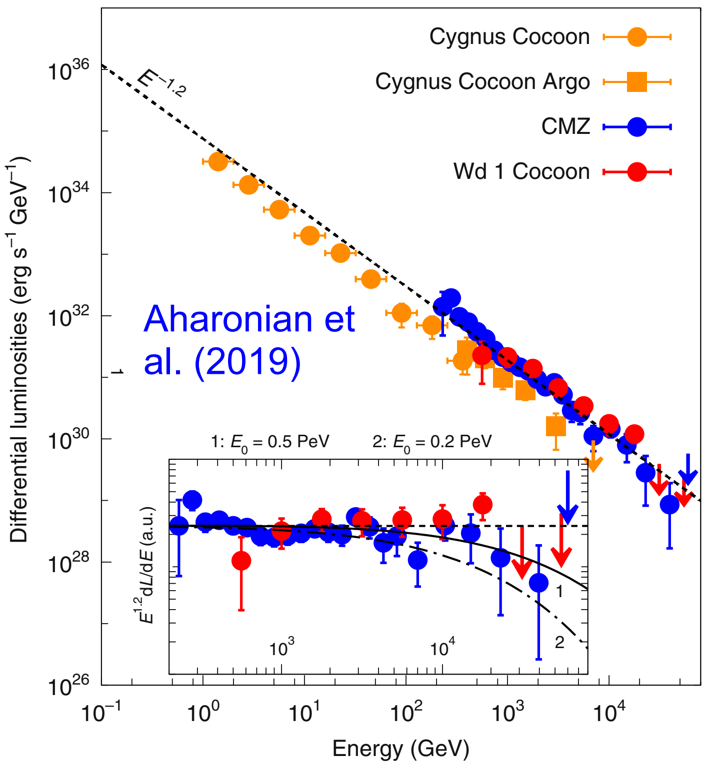

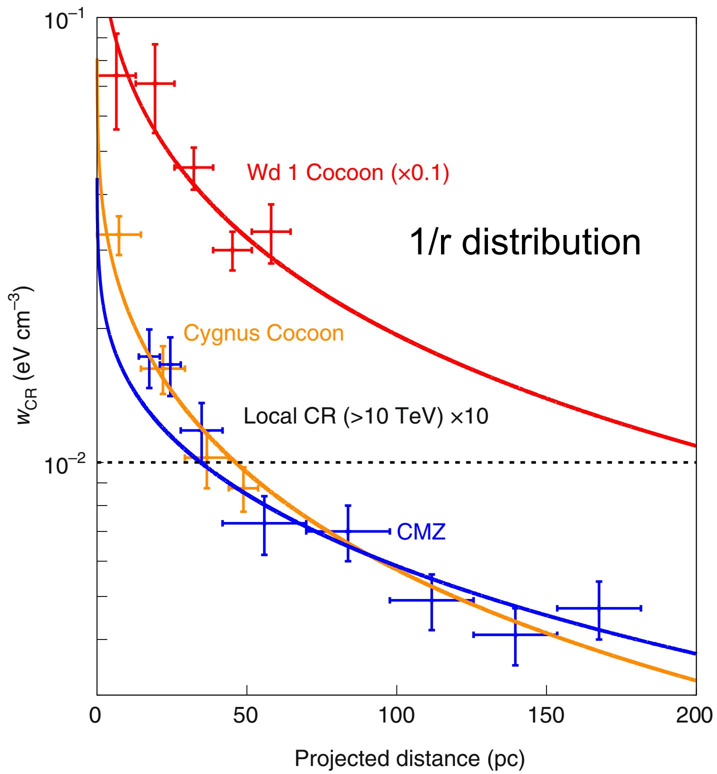

4. Lessons from the cosmic-ray composition

4. Galactic cosmic-ray composition

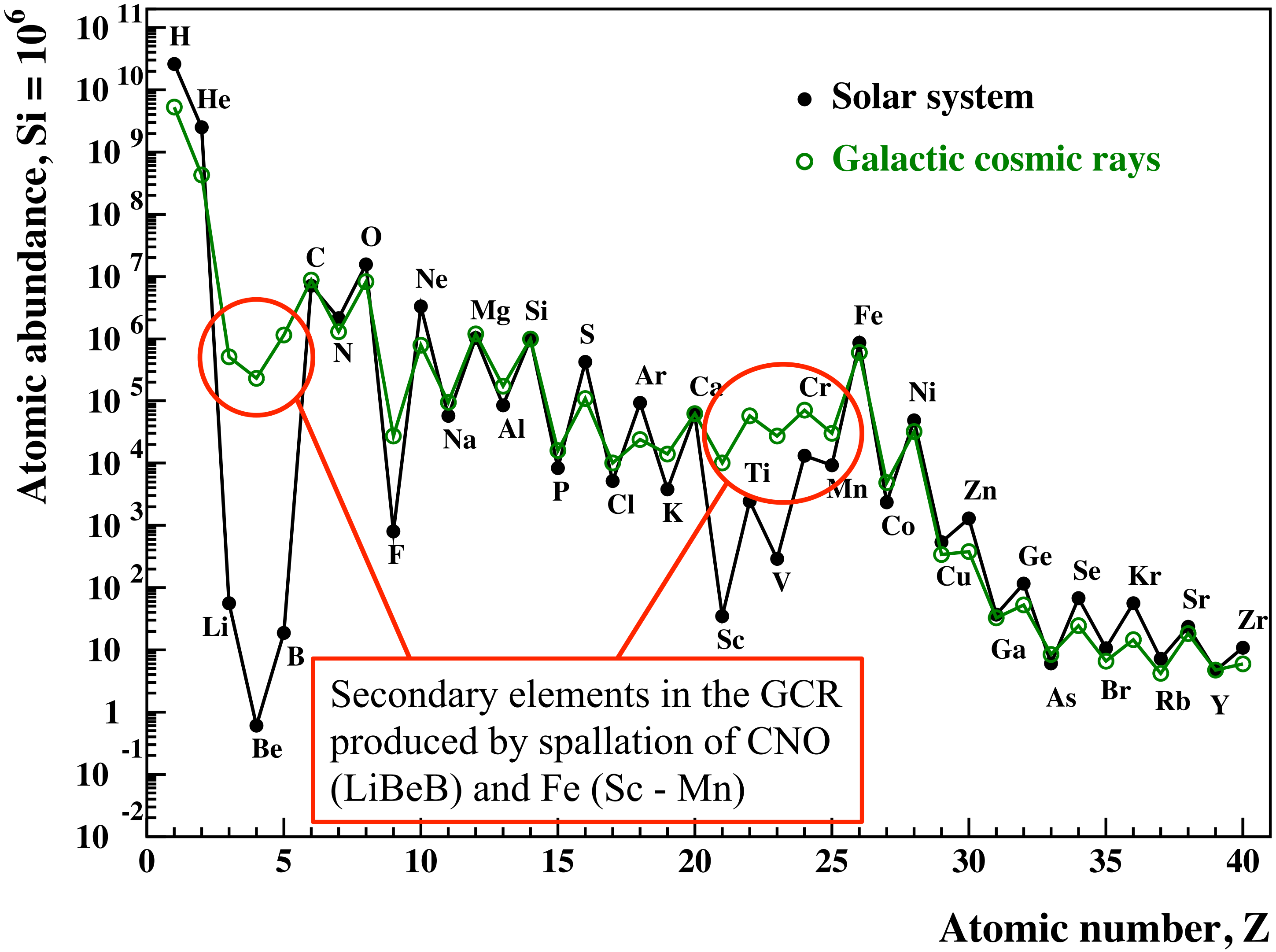

- First order: CR compo. close to solar, but overabundance of secondary elements

4. GCR grammage and lifetime

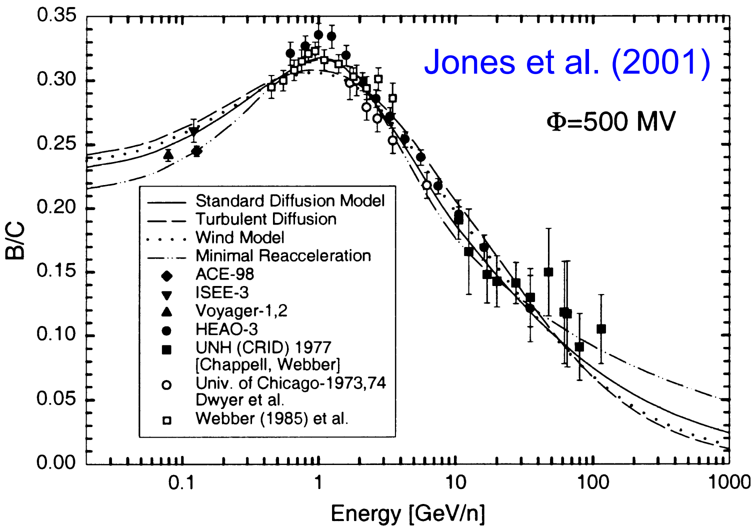

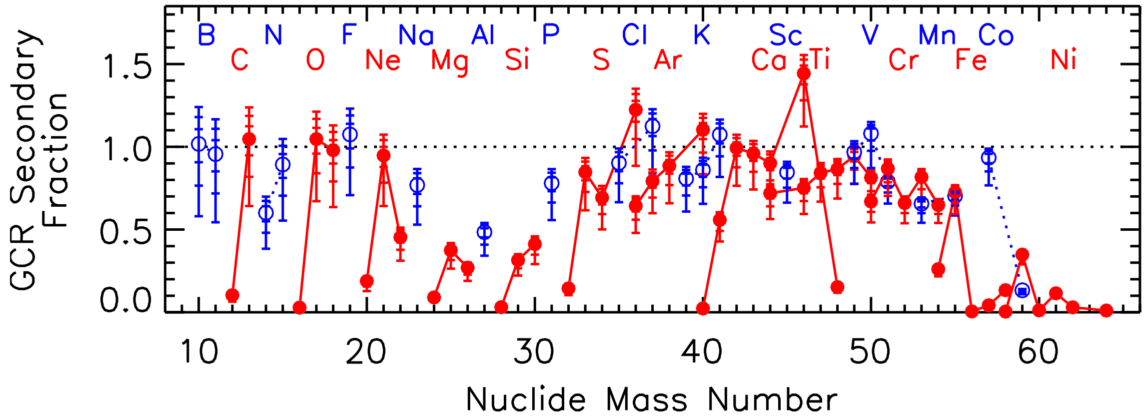

- Model of CR transport constrained with **B/C** (+ other) data (e.g. Génolini et al 2019) ⇒ secondary fractions and **CR abundances at their sources**

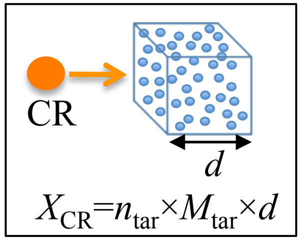

- To produce the measured B/C, the grammage (= target thickness) traversed by CRs is X_{CR} **~ 10 g cm^{-2} at 1 GeV/nucleon**
- The corresponding lifetime of CRs before escape from the Galaxy is

$$\tau_{esc}(1\ \mathrm{GeV}) \sim \frac{X_{CR}}{\rho_{ISM}c} \sim 50\ \mathrm{Myr}$$

where $\rho_{ISM} \sim 2 \times 10^{-25}$ g cm^{-3} is the mean gas density in the CR confinement volume of the Galaxy (disc + halo)

4. GCR source composition

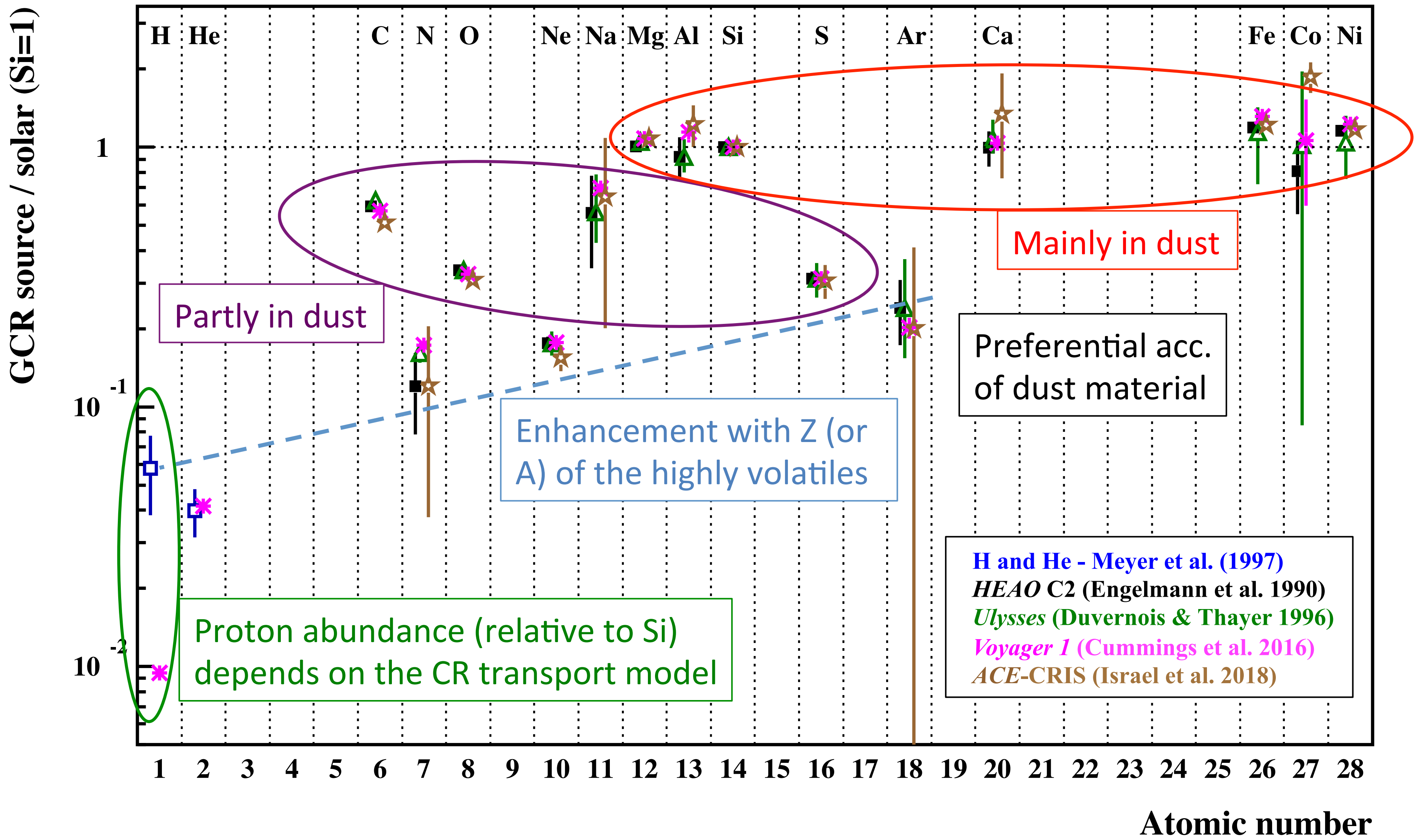

4. Depletion & interstellar dust composition

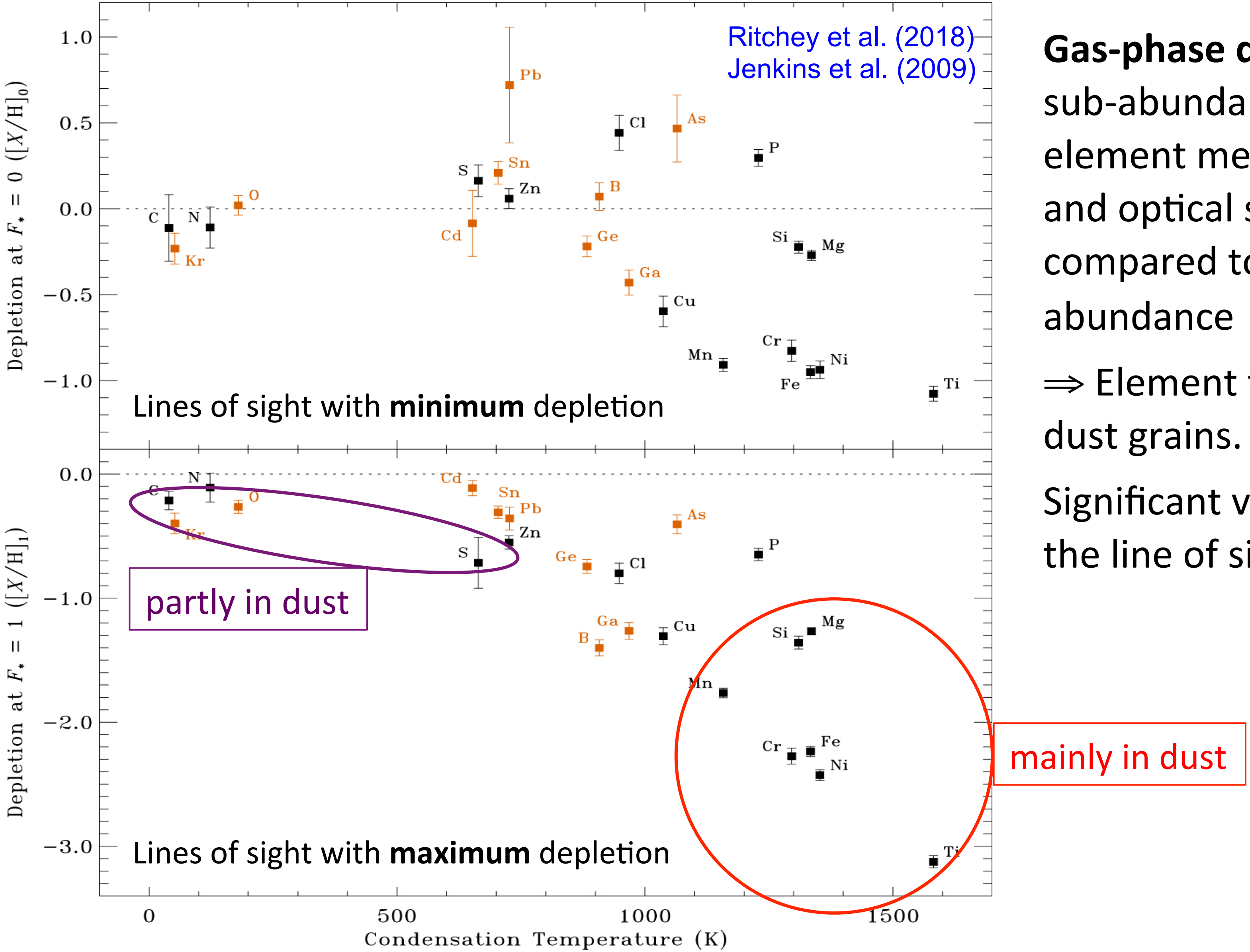

Gas-phase depletion: sub-abundance of an element measured in UV and optical spectroscopy compared to its solar abundance

⇒ Element fraction in dust grains.

Significant variation with the line of sight.

4. A/Q dependence of the acceleration efficiency

- Hybrid (kinetic ions-fluid electrons) simulations of **chemical enhancements** in shock-accelerated ions (Caprioli et al 2017): $C_i \propto (A_i/Q_i)^2$ (Q_i: atomic charge of ion *i*)
- In the hot ISM phase ($T \sim 10^6$ K), $A_i/Q_i \propto \sim A_i^{0.4}$ (partial ionization of heavy ions) $\Rightarrow$ **enhancement with mass of the highly volatiles**
- **Preferential acceleration of grain material** (Meyer et al. 1997), as grain can have huge $A/Q \sim 10^4$ - 10^8 !
  - i. Maximum kinetic energy per nucl. of the accelerated grains (Ellison et al. 1997):

$$\left(\frac{E}{A}\right)_{G,\max} \simeq 100\eta^{-2/3}\left(\frac{V_{sk}}{400\ \mathrm{km\ s^{-1}}}\right)^{4/3}\left(\frac{a}{10^{-7}\ \mathrm{m}}\right)^{-2/3}\times$$
$$\times\left(\frac{n_{\mathrm{H}}}{1\ \mathrm{cm^{-3}}}\right)^{-2/3}\left(\frac{\phi}{10\ \mathrm{V}}\right)^{2/3}\left(\frac{B}{3\ \mu\mathrm{G}}\right)^{2/3}\ \mathrm{keV}$$

  - ii. **Grain sputtering** with ambient gas atoms
  - iii. **Injection of the sputtered ions** in the shock acceleration process with the same (suprathermal) velocity of the parent grain

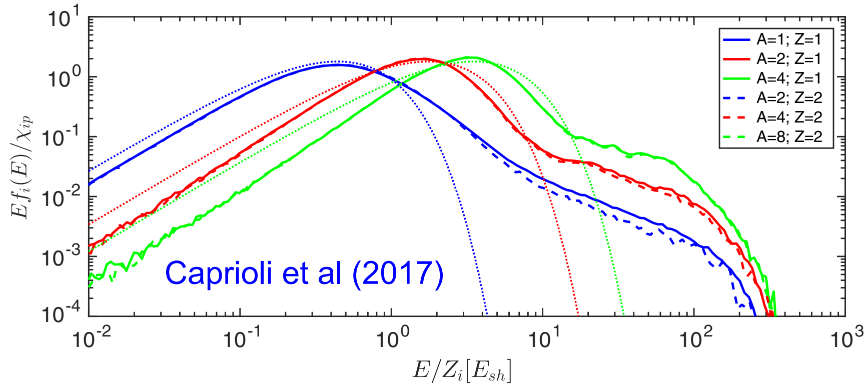

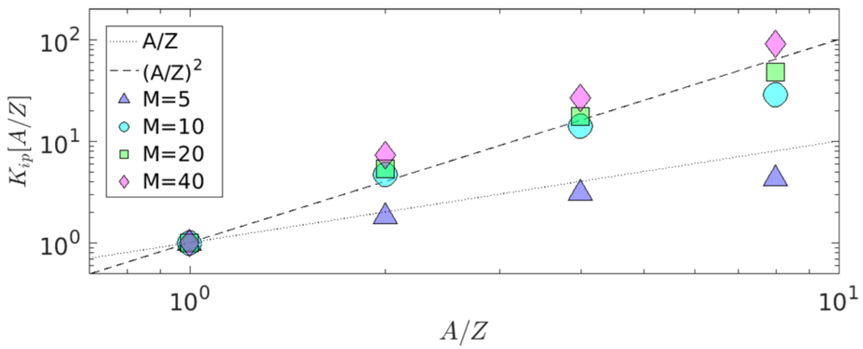

4. GCR isotopic composition - ^{22}Ne

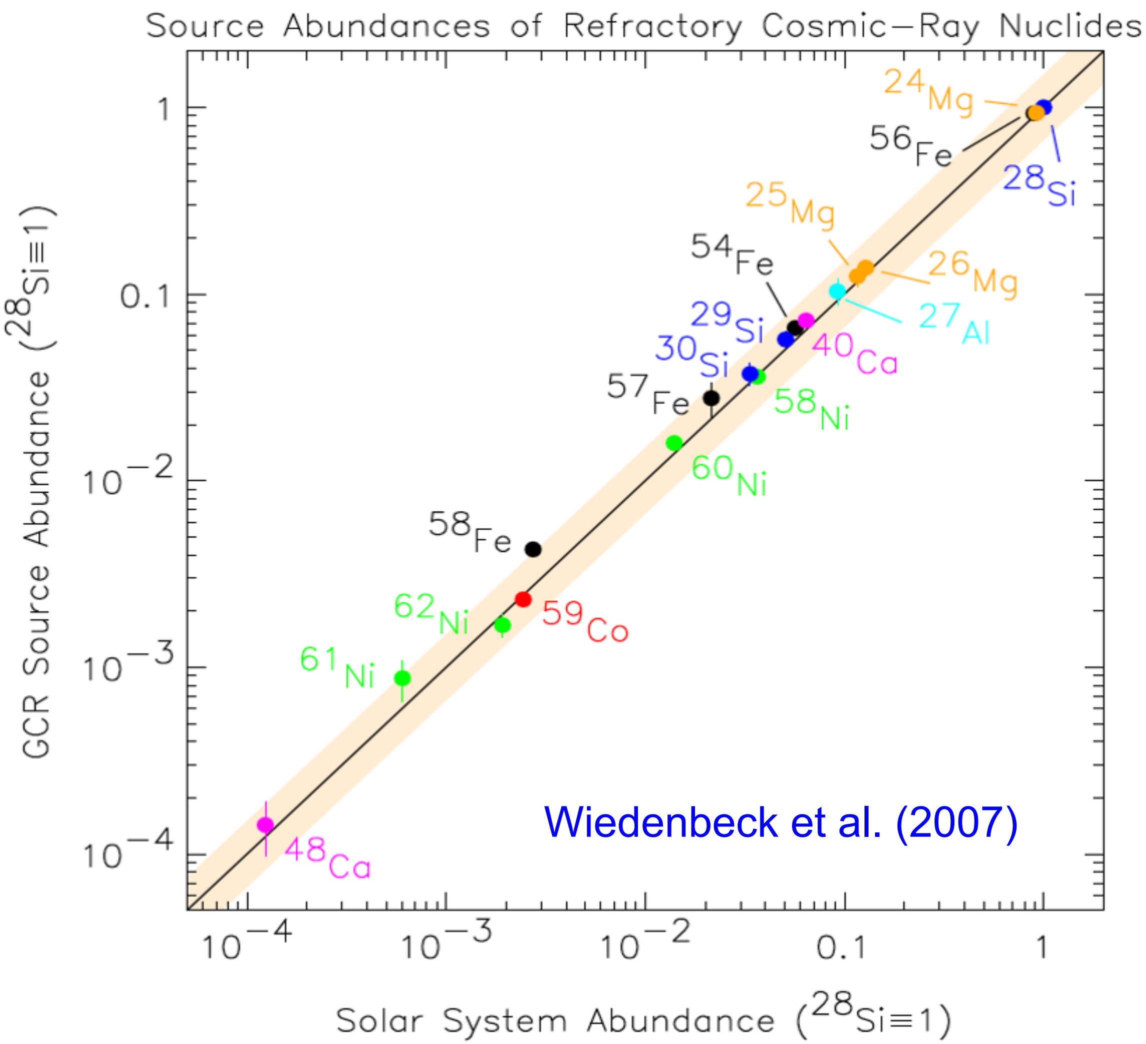

- **Isotopic composition** of refractory CRs also very close to solar: evidence for **acceleration of the average ISM enriched by Galactic chemical evolution** (see VT & Gabici 2018)

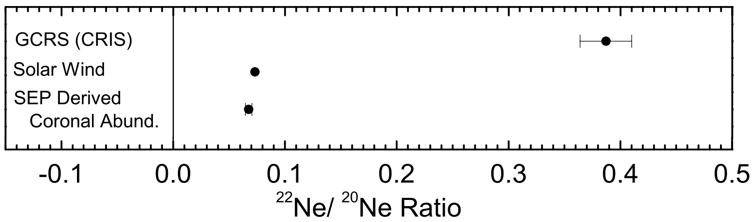

- **High isotopic ^{22}Ne/^{20}Ne ratio** (Garcia-Munoz et al. 1970, Wiedenbeck & Greiner 1981, Binns et al. 2005) = 0.387 ± 0.007 (stat.) ± 0.002 (syst.), which is **5.3 ± 0.3 times the solar ratio** (in the solar wind)!

4. Stellar nucleosynthesis of ^{22}Ne

- ^{22}Ne synthesized by burning of ^{14}N (ashes of CNO cycle) during the **He burning phase**: $^{14}N(\alpha,\gamma)^{18}F(\beta^+)^{18}O(\alpha,\gamma)^{22}Ne$
- Contribution to Galactic CRs of **Wolf-Rayet wind material** expelled during the WC and WO stages? (Cassé & Paul 1982)
- GCR origin in **superbubbles** enriched in ^{22}Ne from winds of massive stars?

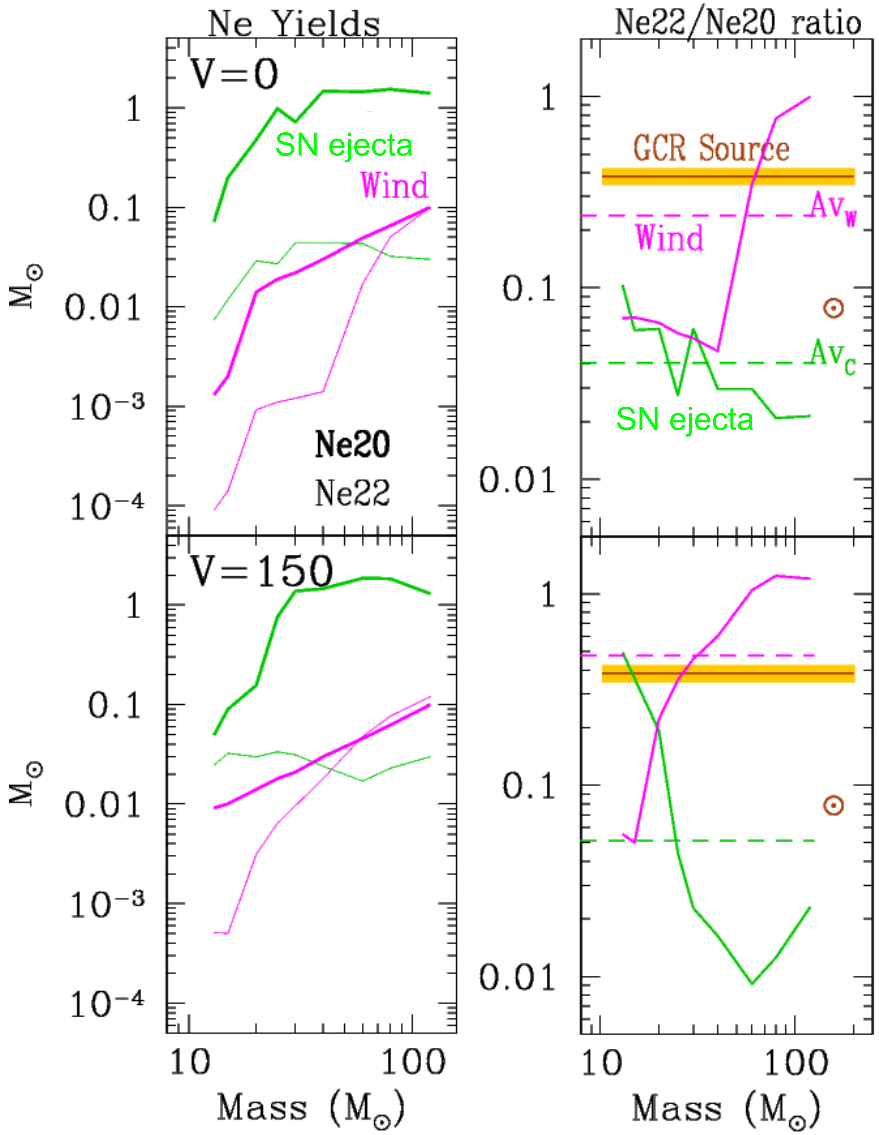

©N. Prantzos, yields from LC2018

4. GCR isotopic composition - ^{60}Fe

- Detection with **16.8 years of data of ACE/CRIS** of **15 nuclei of ^{60}Fe (lifetime τ_{60}=3.8 Myr)** and 2.95×10^5 ^{56}Fe (in ~50 - 500 MeV/nucl.) (Binns et al. 2016)

- ~1 ^{60}Fe could be a secondary CR (fragmentation of ^{62}Ni or ^{64}Ni), ~1 ± ~1 ^{60}Fe could be produced by interaction of heavier ions in the instrument

⇒ **^{60}Fe/^{56}Fe = (4.6 ± 1.7) × 10^{-5}** at top of the detector

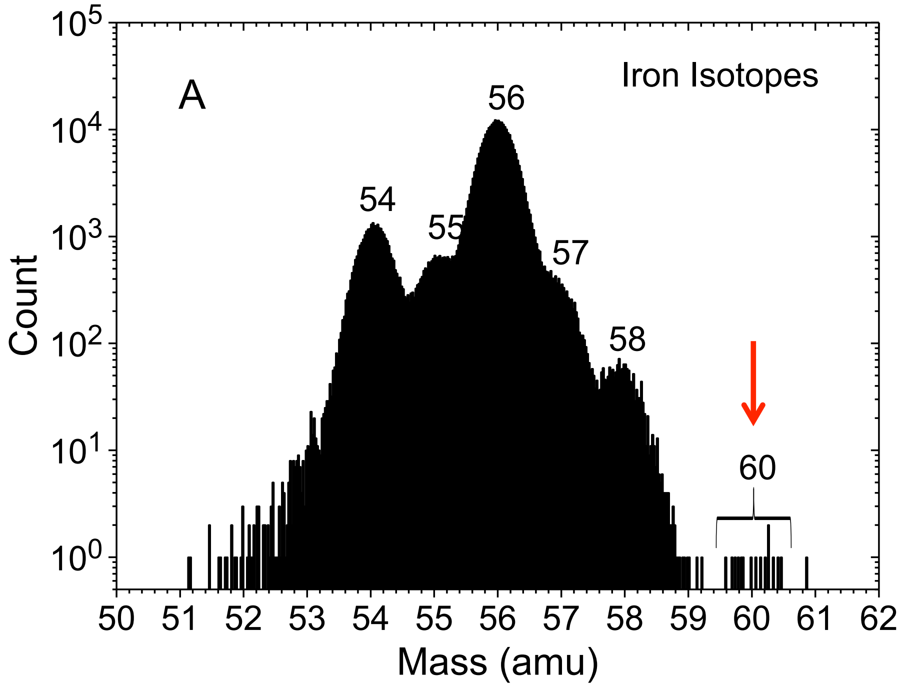

- At the CR source: ^{60}Fe/^{56}Fe = (7.5 ± 2.9) × 10^{-5} (leaky-box model; Binns et al. 2016) or **^{60}Fe/^{56}Fe = (4 ÷ 11) × 10^{-5}** (disk/halo diffusion model; Morlino & Amato 2019)

- Approximate mean distance to the source: **$L \sim (D\,\gamma\,\tau_{60})^{1/2} \sim 400 \div 700$ pc (i.e. local)** where $D \sim (1 \div 3) \times 10^{28}$ cm^2 s^{-1} is the CR diffusion coefficient at ~300 MeV/nucl (e.g. Evoli et al. 2019, Génolini et al. 2019) and $\gamma = 1.3$ is the Lorentz factor

4. Stellar nucleosynthesis of ^{60}Fe

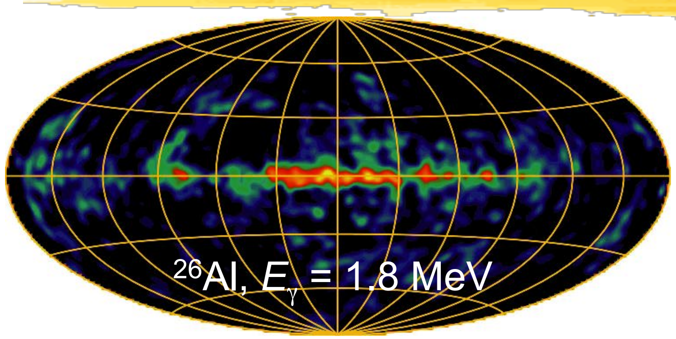

- Average ratio in the Galaxy from γ-ray measurements (INTEGRAL satellite; E_γ = 1.17 & 1.13 MeV from ^{60}Co decay): **(^{60}Fe/^{56}Fe)$_{ISM}$ = 1.5 x 10^{-7}** (see Diehl 2013)

⇒ **^{60}Fe CRs not from the average ISM!**

- ^{60}Fe produced in core-collapse SNe, by neutron capture (i.e. ^{59}Fe(n,γ)^{60}Fe) ⇒ a fraction of the CR material come from **fresh (< a few Myr) SN ejecta**
- ^{60}Fe acceleration at the reverse shock?
- **^{60}Fe acceleration by the forward shock of a nearby SN in a superbubble** (?)

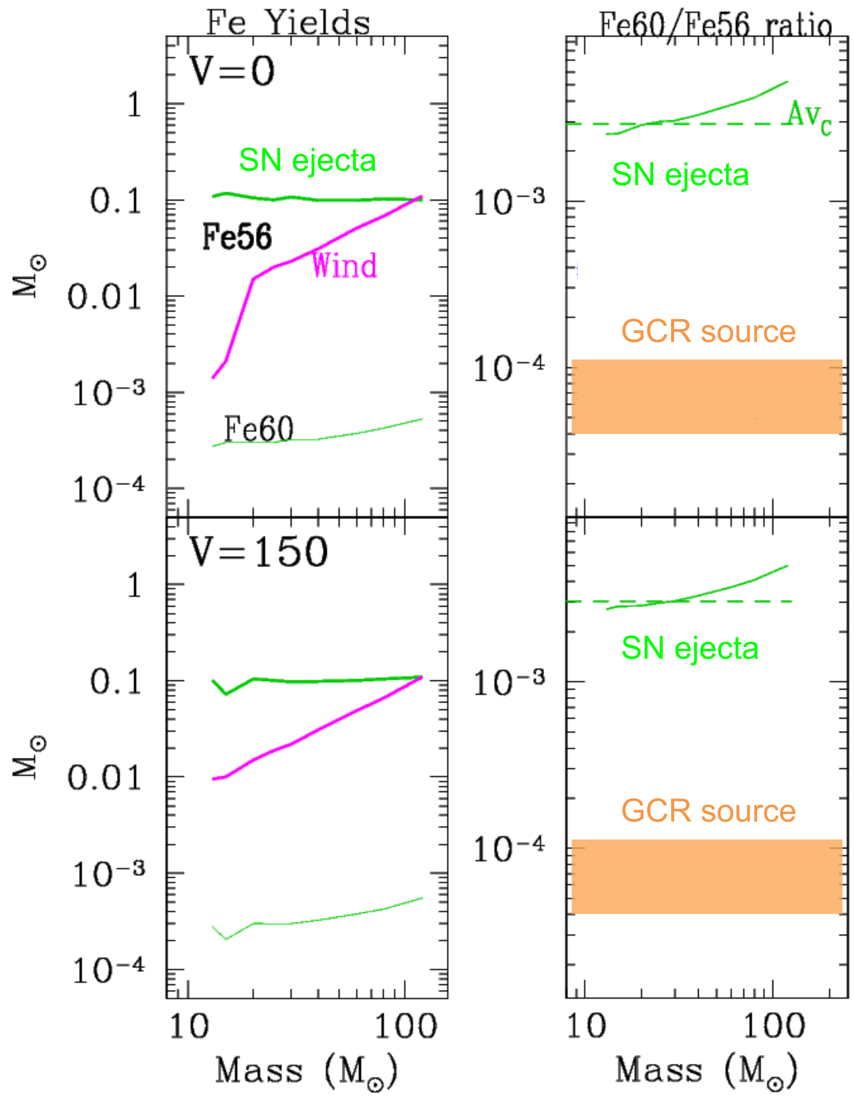

©N. Prantzos, yields from LC2018

4. Local source of cosmic rays

- **Gould Belt**: ring of stars with several OB associations at ~ 120 - 450 pc from the Sun (Gould 1879)
- About 17-20 supernovae (SNe) per million years (Myr) formed in the **Gould Belt** during the past several Myr (Grenier 2004; Frisch & Dwarkadas 2017)
- **Local Bubble**: cavity ($n \sim 0.05$ H cm^{-3}) surrounding the solar system. Originated from 14 - 20 SNe within a moving group now in the Scorpius-Centaurus stellar association (e.g. Breitschwerdt et al. 2016)
- **^{60}Fe detected in deep-sea crusts** suggest two nearby (< 100 pc) and recent SNe: 6.5 - 8.7 Myr and **1.5 - 3.2 Myr** ago (Wallner et al. 2016)

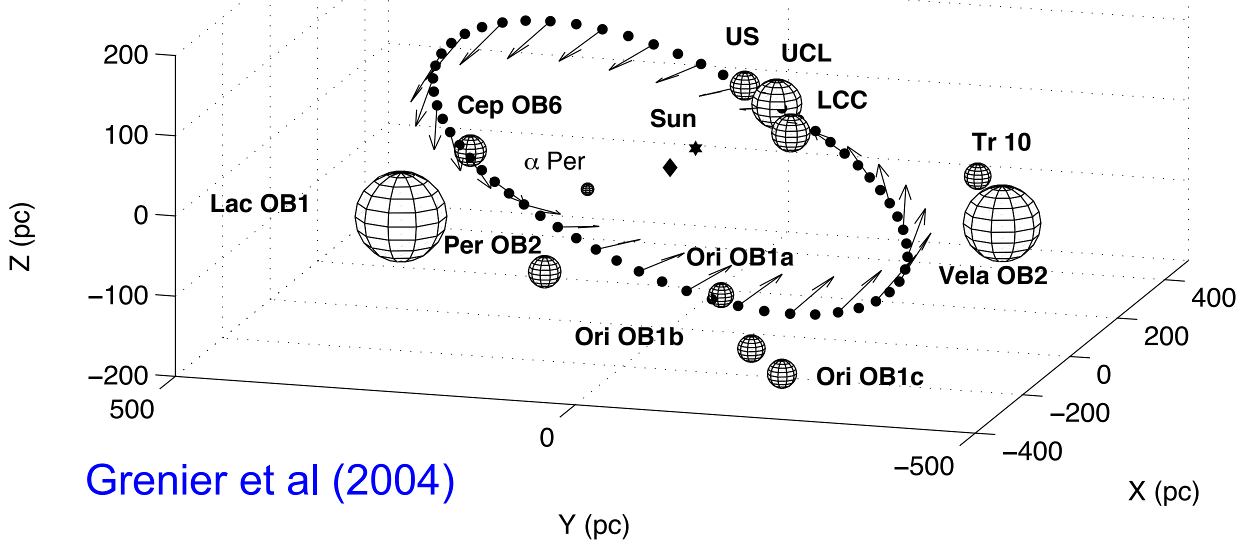

Grenier et al (2004)

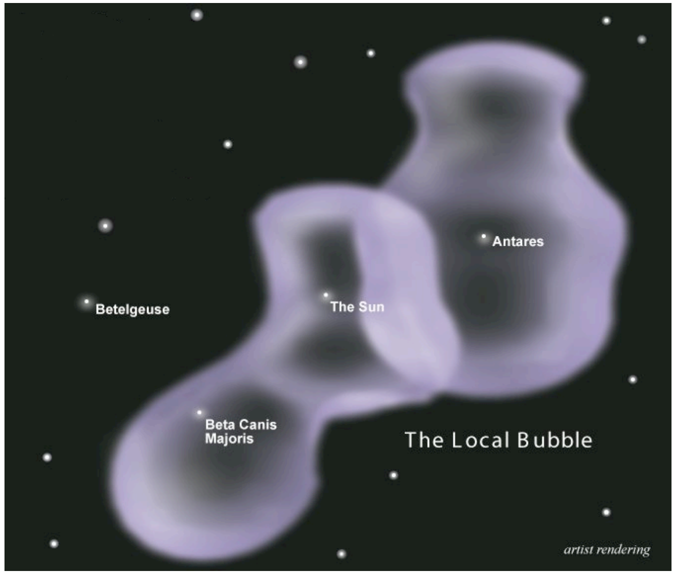

4. Scorpius-Centaurus association

- **Nearest OB association**: subgroup mean distance (de Zeeuw et al. 1999) of 118 pc (Lower Centaurus Crux, age 17 Myr), 140 pc (Upper Centaurus-Lupus, 16 Myr) and 145 pc (Upper Scorpius, 11 ± 3 Myr, Pecaut et al. 2012)

- Stellar population: 1000 - 2000 stars in LCC and UCL (Mamajek et al. 2002), 2525 stars in US (from Initial Mass Function; Preibisch & Mamajek 2008)

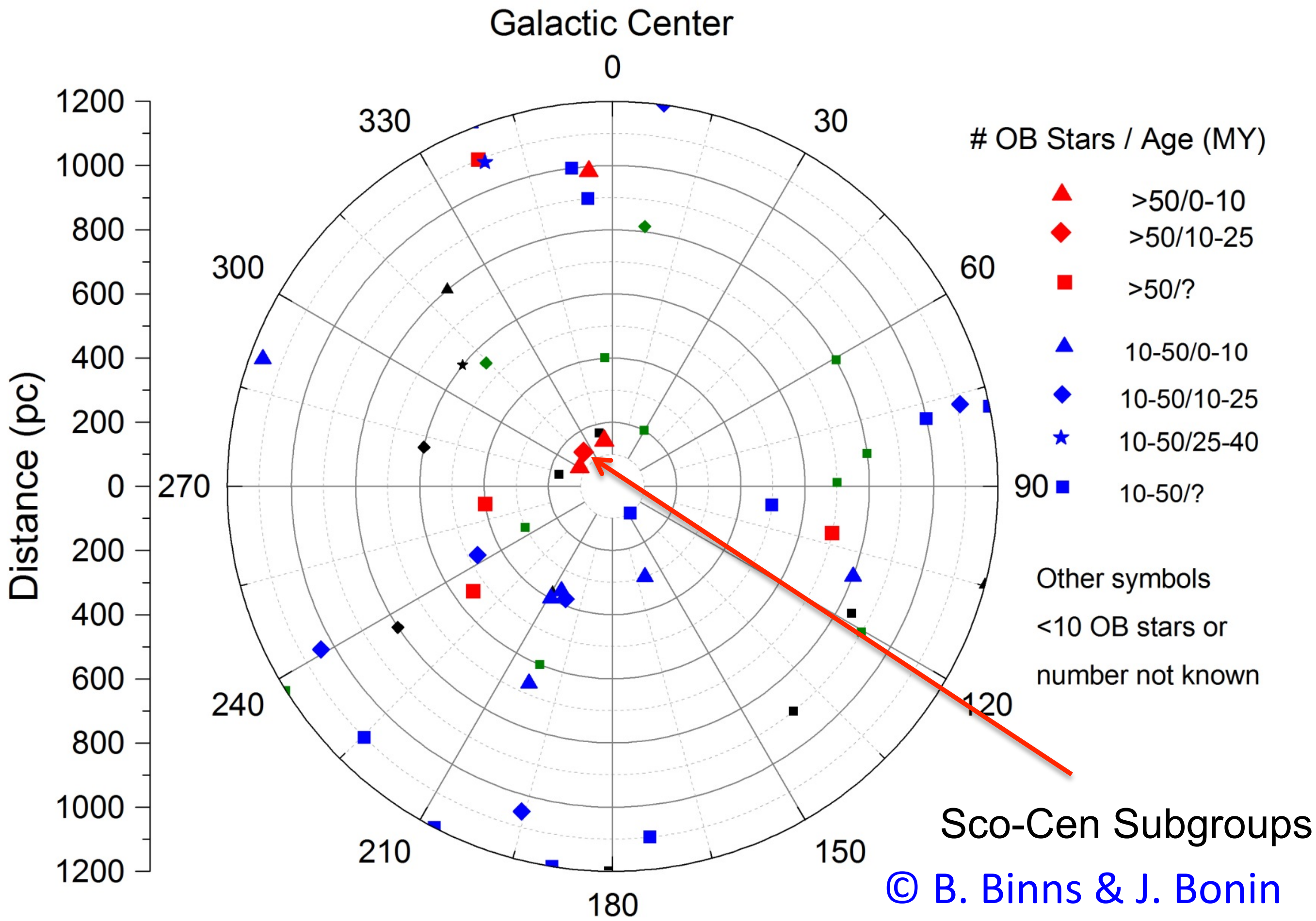

© B. Binns & J. Bonin

4. Scorpius-Centaurus association - age map

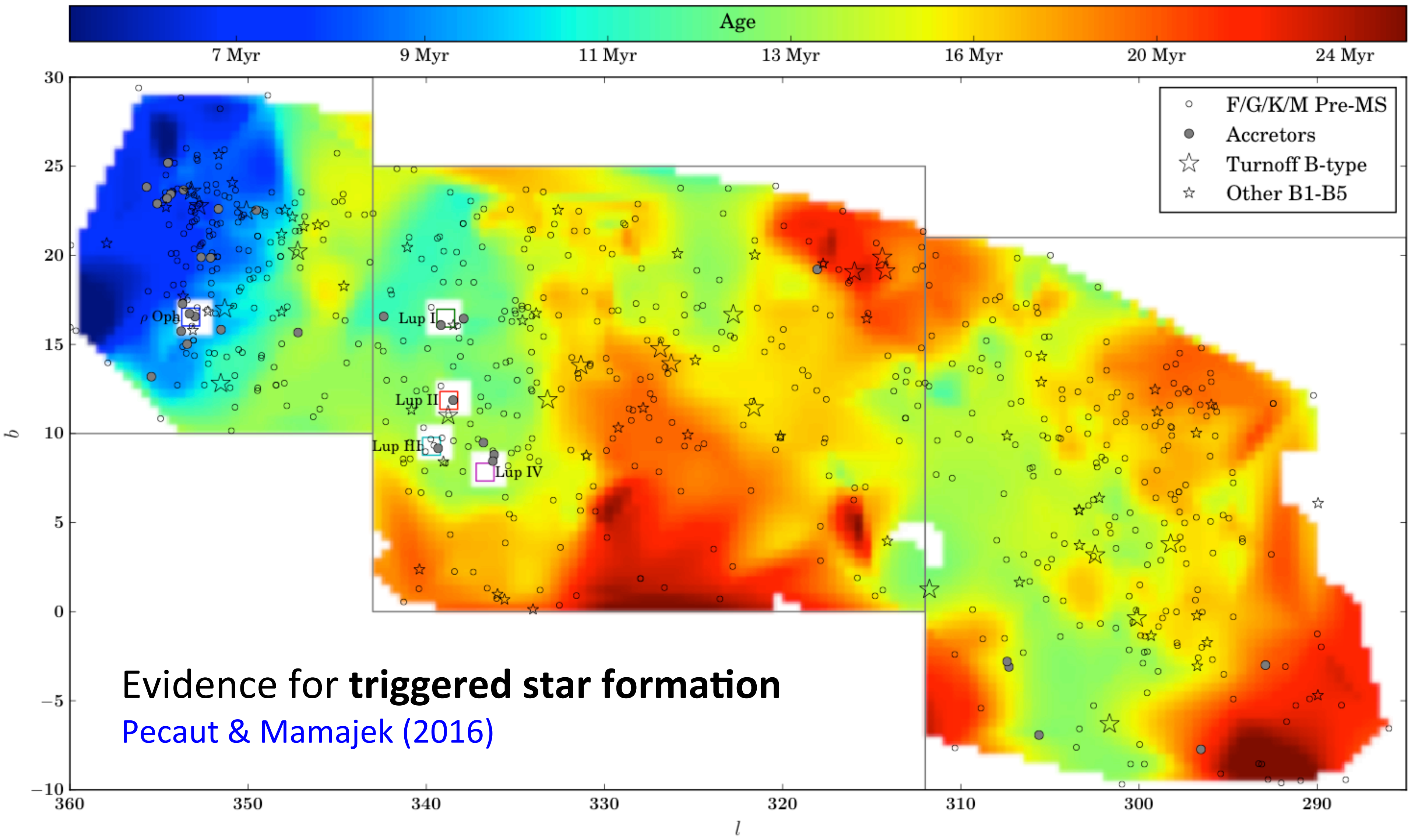

Evidence for **triggered star formation**

Pecaut & Mamajek (2016)

4. Population synthesis in Sco-Cen - Ne and Fe production

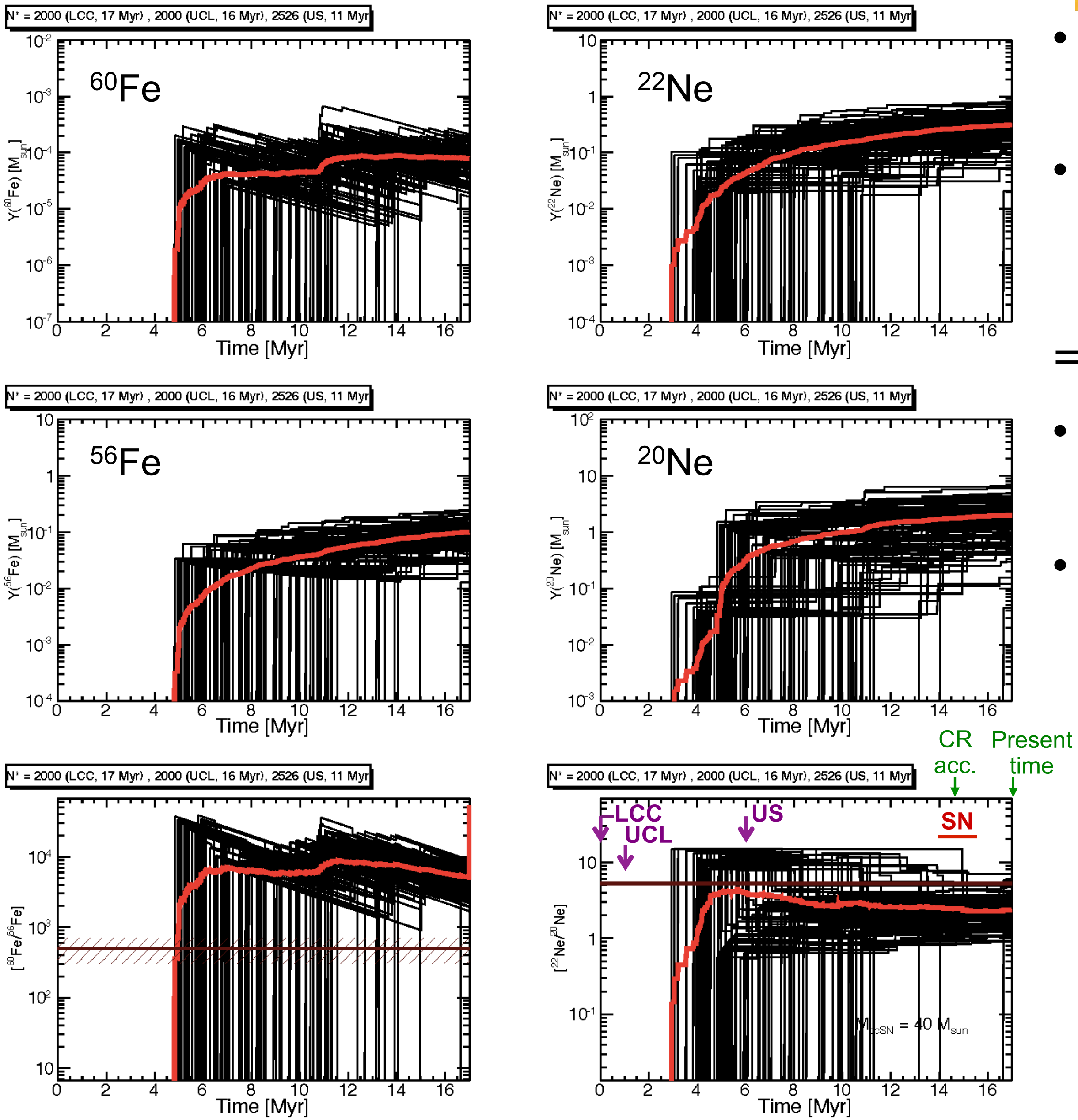

- Stellar masses generated **randomly** (Kroupa et al. 1993)
- **Stars with M > 40 M_{sol} collapse - no SN explosion** (see Sukhbold et al. 2016)

⇒ About **15±5 SNe**

- Stellar yields from Limongi & Chieffi (2018)
- Yield ratios given relative to estimated average values in the ISM:
  - $(^{22}Ne/^{20}Ne)_{ISM} = 7.35 \times 10^{-2}$ (solar wind)
  - $(^{60}Fe/^{56}Fe)_{ISM} = 1.5 \times 10^{-7}$ (gamma-ray astronomy; INTEGRAL)

N. De Séréville & VT, in prep.

4. ^{22}Ne and ^{60}Fe CR from a recent SN in the LB

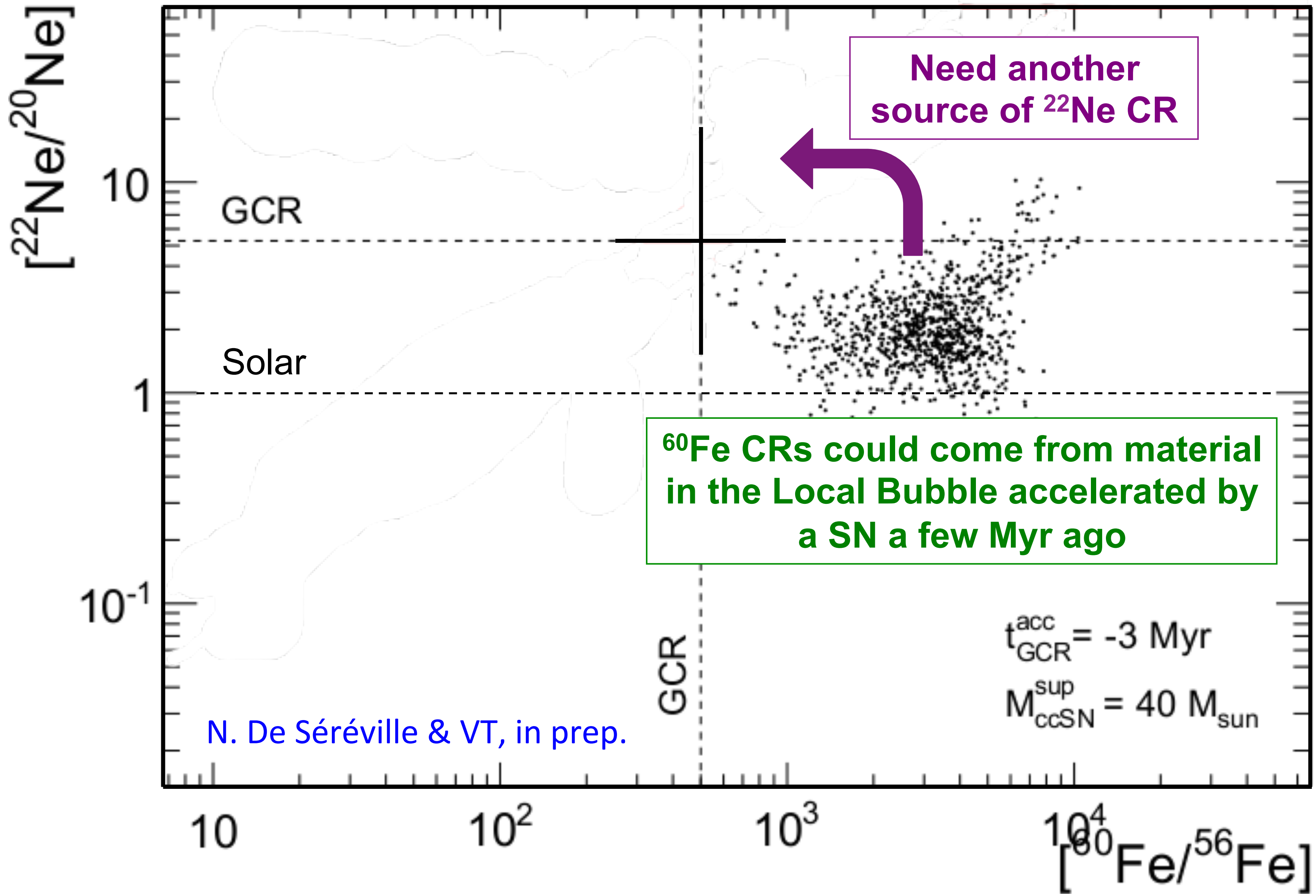

4. ^{22}Ne-enriched CRs from (compact) star clusters?

- From 1D hydro simulations: (i) **wind termination shocks** (WTSs) process $>25\%$ of the total mechanical energy in a star cluster and (ii) a large fraction ($\approx 2/3 - 6/7$) of the total energy processed by WTS and SN shocks goes into **acceleration of wind material enriched in ^{22}Ne** (Gupta et al. 2019)

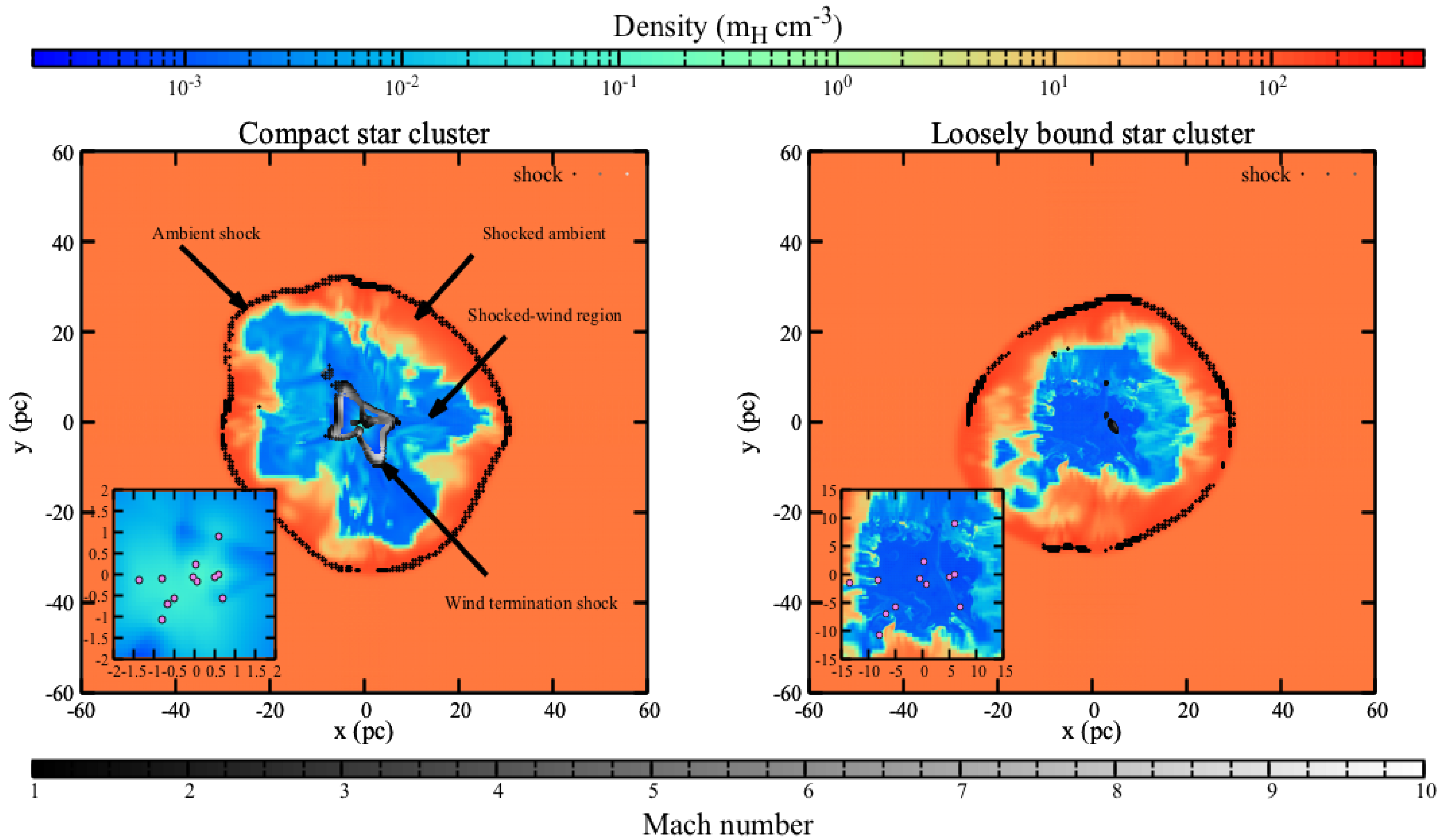

Conclusions

1. **Supernova remnant shocks** accelerate cosmic rays **with about the required efficiency** to explain the Galactic CR energy budget,

2. But they seem **unable to account for** the CR data at **the "knee"** energy and beyond

3. CR acceleration in **(compact) clusters of massive stars might** explain the CR data **beyond the knee** and the **high ^{22}Ne/^{20}Ne ratio**

4. **^{60}Fe CRs** could come from acceleration of material in the Local Hot Bubble enriched by the activity of the **nearby Sco-Cen association**

- Understanding the origin of cosmic rays requires determining the relative contribution of these sources as a function of energy...